Tectonophysics 654 (2015) 75–95

Contents lists available at ScienceDirect

Tectonophysics

journal homepage: www.elsevier.com/locate/tecto

The tectonic evolution of the southeastern Terceira Rift/São Miguel region (Azores)

B.J. Weiß [a,*], C. Hübscher [a], T. Lüdmann [b]

[a] Institute of Geophysics, University of Hamburg, Bundesstrasse 55, D-20146 Hamburg, Germany
[b] Institute of Geology, University of Hamburg, Bundesstrasse 55, D-20146 Hamburg, Germany

ARTICLE INFO

Article history:
Received 17 September 2014
Received in revised form 29 April 2015
Accepted 30 April 2015
Available online 13 May 2015

Keywords:
Azores
Bathymetry
Seismic stratigraphy
Multi-channel seismics
Tectonics

ABSTRACT

The eastern Azores Archipelago with São Miguel being the dominant subaerial structure is located at the intersection of an oceanic rift (Terceira Rift) with a major transform fault (Gloria Fault) representing the westernmost part of the Nubian–Eurasian plate boundary. The evolution of islands, bathymetric highs and basin margins involves strong volcanism, but the controlling geodynamic and tectonic processes are currently under debate. In order to study this evolution, multibeam bathymetry and marine seismic reflection data were collected to image faults and stratigraphy. The basins of the southeastern Terceira Rift are rift valleys whose southwestern and northeastern margins are defined by few major normal faults and several minor normal faults, respectively. Since São Miguel in between the rift valleys shows an unusual W–E orientation, it is supposed to be located on a leaky transform. South of the island and separated by a N120° trending graben system, the Monacco Bank represents a N160° oriented flat topped volcanic ridge dominated by tilted fault blocks. Up to six seismic units are interpreted for each basin. Although volcanic ridges hamper a direct linking of depositional strata between the rift and adjacent basins, the individual seismic stratigraphic units have distinct characteristics. Using these units to provide a consistent relative chrono-stratigraphic scheme for the entire study area, we suggest that the evolution of the southeastern Terceira Rift occurred in two stages. Considering age constrains from previous studies, we conclude that N140° structures developed orthogonal to the SW–NE direction of plate-tectonic extension before ~10 Ma. The N160° trending volcanic ridges and faults developed later as the plate tectonic spreading direction changed to WSW–ENE. Hence, the evolution of the southeastern Terceira Rift domain is predominantly controlled by plate kinematics and lithospheric stress forming a kind of a re-organized rift system.

1. Introduction

The Azores Archipelago is located at the Mid-Atlantic Ridge (MAR) where three major lithospheric plates converge (Fig. 1): the North American Plate in the west and the Eurasian & Nubian plates in the east, the last two separated from each other by a major transform fault (Gloria Fault). MAR and Gloria Fault are linked by an oblique oceanic rift system (Terceira Rift), which is accommodating dextral transtension in WSW–ENE direction caused by the relative movement of the Eurasian and Nubian plates (DeMets et al., 2010; Fernandes et al., 2006). Northward migration of the triple point and the evolution of the present-day Terceira Rift involved increased volcanism/magmatism causing the formation of the Azores Plateau (e.g. Georgen and Sankar, 2010; Luis et al., 1998), a prominent morphological high with an abnormal low water depth of ~2000 m. The volcanic islands at the northeastern rim of the Azores Plateau represent the present-day subaerial volcanism. Hence, the Terceira Rift resembles e.g. the Spiess Ridge in the South Atlantic in terms of a volcanically active and oblique rift system linking a spreading axis with a major transform fault (Ligi et al., 1999; Mitchell et al., 2000).

Both, the jump of the triple junction and the strong volcanism are associated with the existence of a hot spot (e.g. Cannat et al., 1999; Gente et al., 2003; Schilling, 1975) or an anomalously volatile-enriched upper mantle (e.g. Bonatti, 1990; Schilling et al., 1980) which once interacted or is still interacting with the MAR. Yet, the initiation of the Azores Plateau evolution correlates with changes in the relative plate movements of Nubia and Eurasia (Luis and Miranda, 2008) and the increased volcanism is proposed to be caused by stretching of the lithosphere (e.g. Luis et al., 1994; Marques et al., 2013, 2014a; Métrich et al., 2014). Hence, it is still up for debate if the tectonic evolution of the elevated seafloor and the volcanic ridges is mainly controlled by upper mantle processes or induced by lithospheric stress due to tectonic plate kinematics.

In this context, the presented study aims for a deeper insight in the geological evolution of the southeastern Terceira Rift and its submarine basins and highs in time and space. Based on a unique high resolution bathymetric and seismic 2D multichannel data set, we mapped the complex submarine fault systems and identified a seismic stratigraphy for the sedimentary basins in the São Miguel region. Therefore, the first objective is to describe the submarine faults and volcanic ridges

* Corresponding author. Tel.: +49 40 42838 6369; fax: +49 40 42838 5441.
E-mail address: benedikt.weiss@zmaw.de (B.J. Weiß).

http://dx.doi.org/10.1016/j.tecto.2015.04.018
0040-1951/

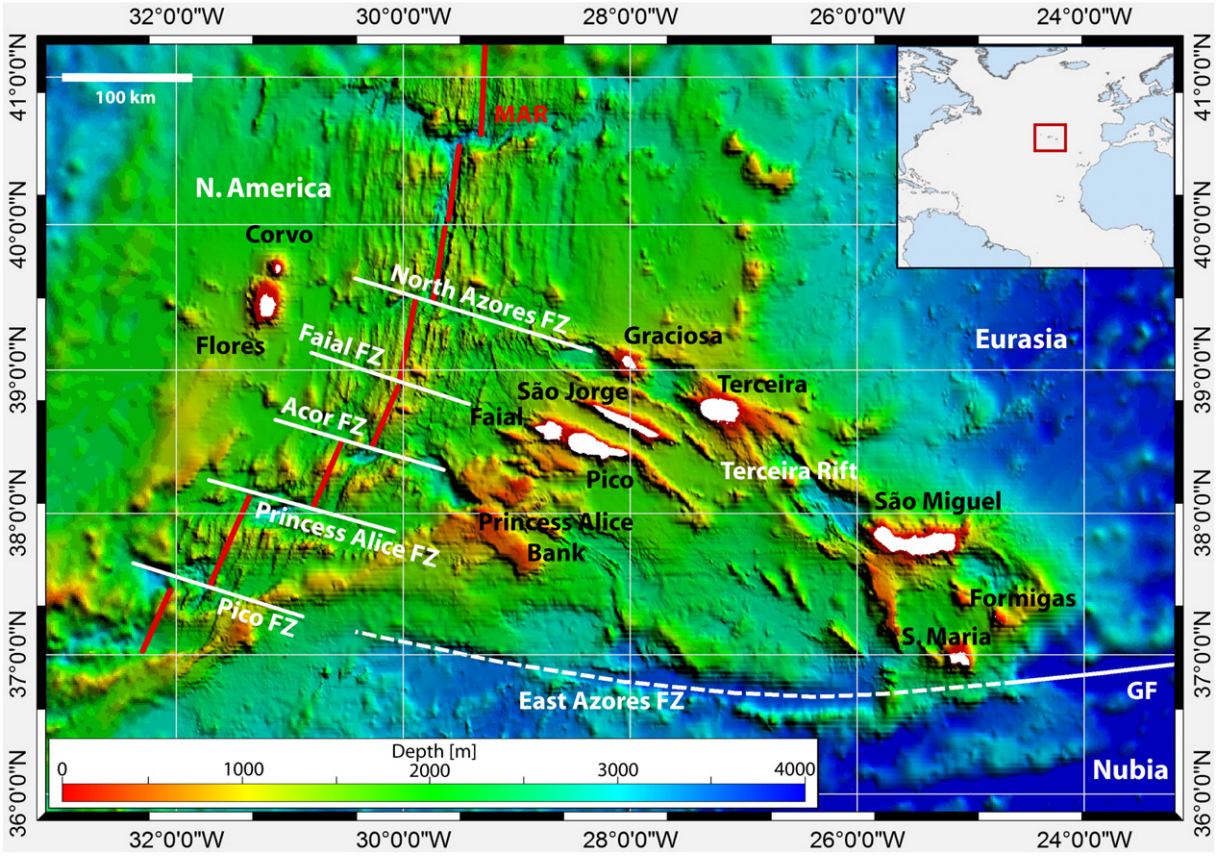

Fig. 1. Azores Plateau and corresponding structures. MAR: Mid-Atlantic Ridge; GF: Gloria Fault; FZ: Fracture Zone. Bathymetric data from Lourenço et al. (1998) and ETOPO1 from Amante and Eakins (2009). Structural features after Luis et al. (1994).

before distinguishing between different sedimentation conditions and the corresponding tectonic and/or volcanic processes. The different stratigraphic sequences then have to be correlated between the basins. This will allow us to evaluate a relative chronology of tectonic and volcanic processes in the working area, which will ultimately result in an evolutionary model for the southeastern Terceira Rift. Finally, general implications will be drawn in terms of structural development and nature of the whole Azores Plate Boundary.

2. Geological context

2.1. Terceira Rift & Azores Triple Junction

The Azores Archipelago consists of 9 islands (Fig. 1). The two westernmost islands (Corvo, Flores) are located on present-day stable North American Plate, whereas the central (Graciosa, Terceira, São Jorge, Faial, Pico) and eastern islands (São Miguel, Santa Maria, Formigas Islets) are distributed along the Nubian–Eurasian plate boundary. The northeastern islands and intercalated basins are known as Terceira Rift, which is defined by the South-Hirondelle Basin, São Miguel Island, the Povoação Basin and the Formigas ensemble in the working area (Fig. 2).

To the South, the East Azores Fracture Zone (EAFZ) forms the southern boundary of the Azores Plateau (Fig. 1) representing the fossil trace of the Gloria Fault on the Nubian Plate (Krause and Watkins, 1970; Luis and Miranda, 2008; McKenzie, 1972; Searle, 1980). At its transition to the Pico Fracture Zone, the EAFZ originally formed the triple point with the MAR in a ridge–fault–fault (RFF) setting. Synchronously to the final stage of the Iberia–Eurasia suture between Oligocene and lower Miocene (33–20 Ma; Luis and Miranda, 2008; Srivastava et al., 1990), the triple point moved northward either in one (Gente et al., 2003; Searle, 1980) or in several steps (Luis et al., 1994; Vogt and Jung, 2004) possibly forming an interim independent Azores Micro Plate (Luis et al., 1994). However, significant extension of 4 mm/a started to occur in the Azores domain at ~20 Ma initiating the evolution of the Terceira Rift in a N50° extensional setting (Luis and Miranda, 2008). While the extension rate is still 4 mm/a (Fernandes et al., 2006), extensional direction rotated from N50° to the present-day ~N70° direction (DeMets et al., 2010) ~10 Ma ago (Luis and Miranda, 2008). Until 7 Ma, the formation of the Terceira Rift involved the accretion of large volumes of extrusives and intrusives as well as underplated material (Cannat et al., 1999; Gente et al., 2003; Luis et al., 1998). This caused the creation of thickened crust (Dias et al., 2007; Georgen and Sankar, 2010; Luis and Neves, 2006; Silveira et al., 2010) referencing to the abnormal elevated seafloor of the Azores Plateau.

Today, the triple junction is located ~150–250 km north of its former position (Fig. 1) forming a diffuse triple junction area between the Acor and North Azores Fracture Zone (Marques et al., 2013, 2014a; Miranda et al., 2014), where the MAR spreading rate increases from 20 in the south to 22 mm/a in the north (DeMets et al., 2010). Further to the east and west of Terceira, extension is mainly accommodated along N110°–120° striking linear volcanic ridges (with São Jorge and Faial/Pico representing an extreme case) and N120°–160° trending faults (e.g. Hildenbrand et al., 2014; Lourenco et al., 1998; Miranda et al., 1998, 2014), which overprint MAR related N15° fabrics. Southeast of Terceira, extension concentrates at the southeastern Terceira Rift, where N140° to N150° trending structures become abruptly prominent (Fernandes et al., 2006; Lourenço et al., 1998; Miranda et al., 1998). These different trends are assumed to be the result of plate boundary effects (Georgen and Sankar, 2010; Neves et al., 2013) and structural heritage (Navarro et al., 2009). They form a diffuse plate boundary consisting of several tectonic blocks (Lourenço et al., 1998; Miranda et al., 1998) and en échelon horst graben structures (Marques et al.,

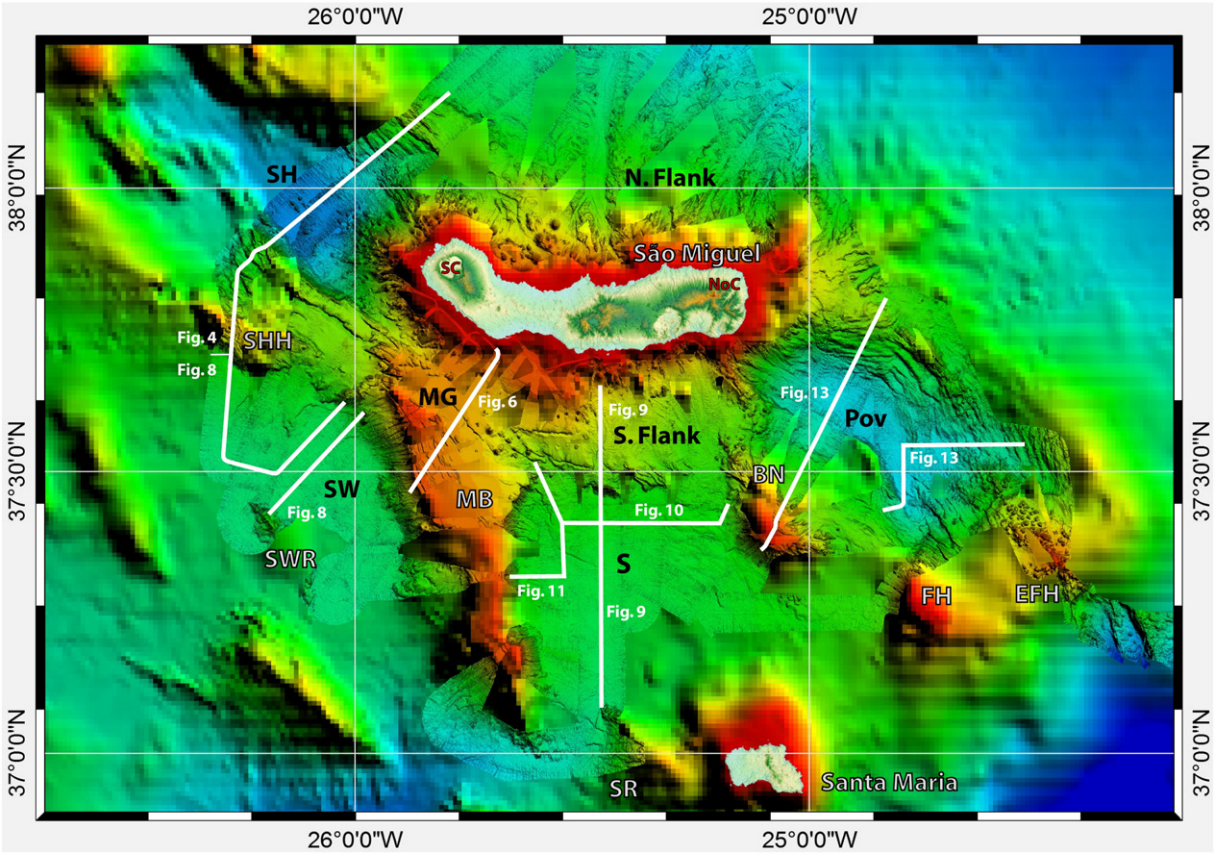

Fig. 2. Deposition centers and structures in the working area and location of seismic profiles shown in this study. Deposition centers (black): SH: South-Hirondelle Basin; MG: Monacco Graben; SW: Southwest Basin; S: South Basin; Pov: Povoação Basin. Submarine highs (white): SHH: South-Hirondelle High; SWR: Southwest Ridge; SR: South Ridge; MB Monacco Bank; BN: Big North High; FH: Formigas High; EFH: East Formigas High. Onshore volcanos (red): SC: Sete Cidades Volcano; NoC: Nordeste Complex.

2013, 2014a; Miranda et al., 2014). Local seismicity is dominated by normal and strike-slip faulting (Borges et al., 2007; Buforn et al., 1988; Grimison and Chen, 1986; Udías et al., 1976) within a right lateral transtensional regime. However, sinistral strike-slip events have been recognized as well (Hirn et al., 1980).

2.2. Upper mantle anomaly

Ridge jump and strong volcanism in the Azores domain are attributed to an interaction of a hot-spot with the MAR by several authors. This coincides with the observation of geochemical anomalies (e.g. Bourdon et al., 2005; Schilling, 1975; White and Schilling, 1978) and an anomalous elevated ridge-axis (e.g. Detrick et al., 1995; Escartín et al., 2001; Schilling, 1985; Thibaud et al., 1998). Based on tomographic studies (e.g. Montelli et al., 2006; Silveira et al., 2006, 2010; Yang et al., 2006), corresponding negative seismic velocity anomalies beneath the Azores are observed. Starting interaction between MAR and a moving hot-spot initiated the northward migration of the triple junction (Vogt and Jung, 2004) and caused enhanced volcanism forming the Azores Plateau. After the hot-spot had passed the ridge, the constructed plateau was rifted and normal seafloor spreading has reestablished (Cannat et al., 1999; Escartín et al., 2001; Gente et al., 2003). Involved mantle upwelling partly accounts for the depth anomaly associated with the Azores Plateau and traction of the mantle flow beneath the lithosphere controls rifting processes along the Terceira Rift (Adam et al., 2013).

In contrast, other authors refer to the fact that the islands are young and do not reflect a hot-spot-track in terms of a clear age progression (Beier et al., 2008). As an alternative, they propose upper mantle domains with an enriched volatile content (Asimow et al., 2004; Bonatti, 1990) or the decompression of a "wet" mantle caused by extensional tectonics (Métrich et al., 2014) to contribute to the enhanced volcanism.

3. Data and methods

This work is based on high resolution bathymetric data and a 2D multichannel seismic data set collected by University of Hamburg scientists on board of *RV METEOR* during cruise M79/2 in 2009 (Hübscher, 2013). The seismic data set consists of profile lines with a total length of 1000 km spread around São Miguel Island. The seismic signals were generated by an array of two GI-Guns with a generator volume of 45 in^3 and an injector volume of 105 in^3 each. For data recording a 600 m long asymmetric digital streamer was used, containing 144 channels with an average increment of 4.2 m. Shots were released every 25 m at a speed of 5 kn. Data processing first encompassed trace editing and CMP sorting with a CMP increment of 5 m. Subsequently, several bandpasses with 10/20/300/400 Hz, spike & noise burst filter, FX-deconvolution and FK-filter were applied before NMO-correction and post stack time migration.

High resolution bathymetric data were synchronously recorded using the Kongsberg EM710 and EM120 Multibeam echosounders installed on board of *RV METEOR*. During processing, navigation errors were interpolated and depths/positions were recomputed using sound velocity profiles. After beam editing was applied for every single swath to eliminate spikes and noisy data, the data was gridded with a spacing of 26 × 26 m. However, since the horizontal accuracy is limited to ~2% of the water depth, effective resolution in water depth higher than 1300 is less. The background bathymetric information is a superposition of a 1 × 1 km grid of data presented by Lourenço et al. (1998), which can be found under http://w3.ualg.

pt/~jluis/acores_plateau.htm, and ETOPO1 data (~1.9 × 1.9 km) published by Amante and Eakins (2009). The topographic data shown is originated from ASTER GDEM, which is a product of METI and NASA.

For this study, faults were picked based on the high resolution bathymetry only. Presented rose diagrams summarize the strikes of fault segments weighted by fault lengths. Counts of picked fault segments are given in the upper left corner of the diagram inset (Figs. 3, 5 and 12). Dip angles of fault scarps were measured based on the EM120/EM710 data using the program *FLEDERMAUS* (© by QPS).

Intervening bathymetric highs and volcanic ridges hamper the direct stratigraphic correlation of the sedimentary basins. Nevertheless, characteristics and geometry of seismic units as well as onlap configurations between them allow us to identify a relative chronology encompassing three major phases in the evolution of the working area. An overview of these evolutionary stages, a brief description of the associated geological processes and the equivalent seismic units are presented in Table 1. Colors of Table 1 match the colors of the corresponding seismic units presented in Figs. 4, 6, 8–11 and 13 as well as the color-code of the sketches in Figs. 13 and 14. Units associated with two major phases are described by a gradual transition of the corresponding colors (e.g. SH2-5b in Fig. 4). The nomenclature of the seismic units is based on the abbreviation of the depositional center (e.g. MG for Monacco Graben). Units of different depositional centers with the same number are associated with the same geological phase of evolution and therefore trace the relative chronology in the working area (see Table 1). Sediment thicknesses are given in milliseconds [ms] throughout the text, since a velocity analysis was not performed during data processing. Assuming interval velocities of 2000 m/s within the sedimentary units, milliseconds are equivalent to meters.

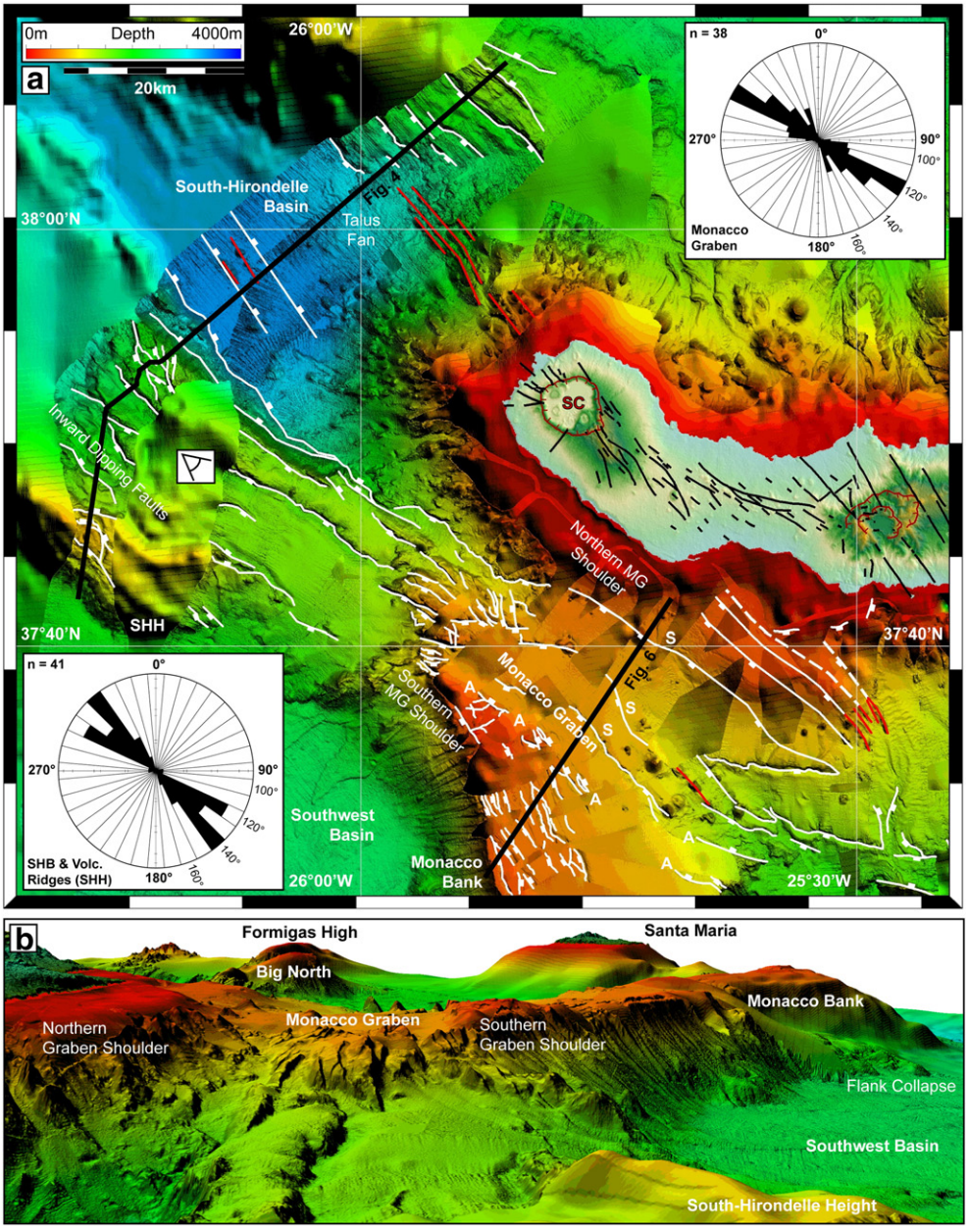

Fig. 3. Bathymetry and picked faults in the western working area (a) and 3D view (b). Monacco Graben is bounded to the south by an antithetic fault A, which also separates N120° and N160° setting. S marks the synthetic normal faults described in the text (a). White line: Fault. Dashed white line: Inferred fault. Red line: Volcanic lineament. Thick black lines indicate seismic profiles. SHB: South-Hirondelle Basin; SHH: South-Hirondelle High. Eye symbol denotes the viewing direction of the bottom 3D sight. Illumination from N90° with an azimuth of 60°.
Onshore faults based on Carvalho et al. (2006), Ferreira (2000) and Queiroz (1997).

Table 1
Overview of the stratigraphic units, seismic horizons and associated evolutionary stages of the southeastern Terceira Rift. Colors indicate the stage of N50°-spreading (blue), the Pre-/Syn-Monacco-Bank stage (purple) and the Post-Monacco-Bank stage (green). Stratigraphic units with two colors could not be correlated with one single stage only. Color code is the same as shown in the line drawings of Figs. 4, 6, 8–11 and 13 as well as in the sketches presented in Figs. 13 and 14.

Evolutionary stage	Seismic horizon	Time [Ma]	Description	M. Graben	SW. Basin	S. Basin	Pov. Basin	S.H. Basin
Stage III			S–Basin first tectonically active, later inactive; subaerial evolution of São Miguel	MG4/5	SW4/5	S5	Pov4/5	SH2/5a SH2/5b SH2/5c
	S	≥0.9	Uniform sedimentation during tectonic quiescence in the S–Basin; tectonic reactivation of the Povoação–Basin			S4		
	R	5.3–4.3?	Formation of Monacco Graben; evolution of early Santa Maria Island?	MG3	SW3	S3		
	Q	≤5.9						
Stage II			Onset of N70° extension; Formation of Monacco Bank; Pov.–Basin inactive; evolution of early Santa Maria Island?	MG2	SW2	S2	Pov2/3	
	P	~10						
Stage I			N50° extension	–	SW1	S1a/S1b	Pov1	SH1

4. Results & interpretation

The working area is dominated by a succession of bathymetric highs (strongly over-printed by tectonism) and basins. Combined descriptions of bathymetric expression, seismic profiles and the resulting stratigraphy are presented for 5 geographical sub-areas treated in an anticlockwise manner around São Miguel (Fig. 2): South-Hirondelle Basin (SH), Monacco Graben (MG) & Monacco Bank (MB), Southwest Basin (SW), South Basin (S) & southern island flank and Povoação Basin (Pov). Images of the high resolution bathymetry (Figs. 3, 5 and 12) without any comments and markings can be found in the supplementary material.

4.1. South-Hirondelle Basin

4.1.1. Observations bathymetry

The bathymetry northwest of São Miguel Island is dominated by the South-Hirondelle Basin (SH) with a maximum water depth of 3250 m (Fig. 3). To the southwest the basin is bordered by a volcanic ridge including the South-Hirondelle High and to the northeast by a further volcanic ridge, both dissected by numerous normal faults with typical vertical offsets of 200/300 m. Fault scarps of the northeastern ridge dip basinwards with 30–45°. Some of the faults apparently reach the submarine flank of Sete Cidades Volcano, where they offer/offered a pathway for magma to ascent resulting in chains of elongated volcanic structures or cones. In contrast, the southwestern ridge is more complex as it is offset by inward dipping faults. Corresponding fault scarps again reveal dip angles of 30°–45°. The basin itself is asymmetric since the northeastern flank shows an average slope angle of 5°, whereas the southwestern flank is formed by two major fault scarps each dipping with 25° to 30° and altogether revealing a vertical offset of 1600 m.

Three dominant strike directions were identified. Faults at the northeastern ridge strike ~N140°. Two faults piercing the seafloor in the basin and the major fault at the lower slope of the southwestern ridge trend ~N150°. On top of the southwestern ridge, again a comparable N140° trend is observable, but interfering with a N120° oriented fault system. These faults continue to the southeast where they merge with the mainly N120° trending Monacco Graben.

4.1.2. Observations seismic

Four distinct seismic units are resolved within the basin (Fig. 4). SH1 represents the acoustic basement and is highly offset by normal faults. The volcanic ridges bordering the basin are both covered by a thin sedimentary unit (SH2-5a), which reveals sub-parallel reflections and masks basement faults south of the data gap. Inside the basin, unit SH2-5b shows distorted and irregular high amplitude reflections where the seafloor slightly dips basinward. Where the seafloor is flat, SH2-5b is characterized by divergent reflections dipping southwest. On top, the small unit SH2-5c is piercing the seafloor. It is characterized by strong chaotic and disrupted reflections.

4.1.3. Combined interpretation of bathymetric and seismic data

Due to the high reflection amplitude, we interpret reflection "P" as the magmatic/volcanic basement (Fig. 4). The lenticular geometry of SH2-5a and the presence of moats adjacent to escarpments in the basement suggest current controlled deposition (Rebesco et al., 2014 and references therein) on top of the rift flanks. The lateral variation of the internal stratification of SH2-5b implies a lateral variation of depositional processes. The northeastern part represents a talus fan. In contrast, the southwestern part is well stratified and shows strong internal reflections implying an obviously alternating acoustic impedance and a vertically alternating succession of turbidites and hemipelagic sediments, respectively. SH2-5c is the southeastern tip of a volcanic lineament (red line within the basin in Fig. 3a) and – consequently – of volcanic origin. The South-Hirondelle Basin represents a graben with dominant N140–150° oriented normal faults within the basin. The divergent reflection pattern of southwestern SH2-5b is a clear evidence for syn-sedimentary tectonics and indicates major vertical movements along the southwestern basin

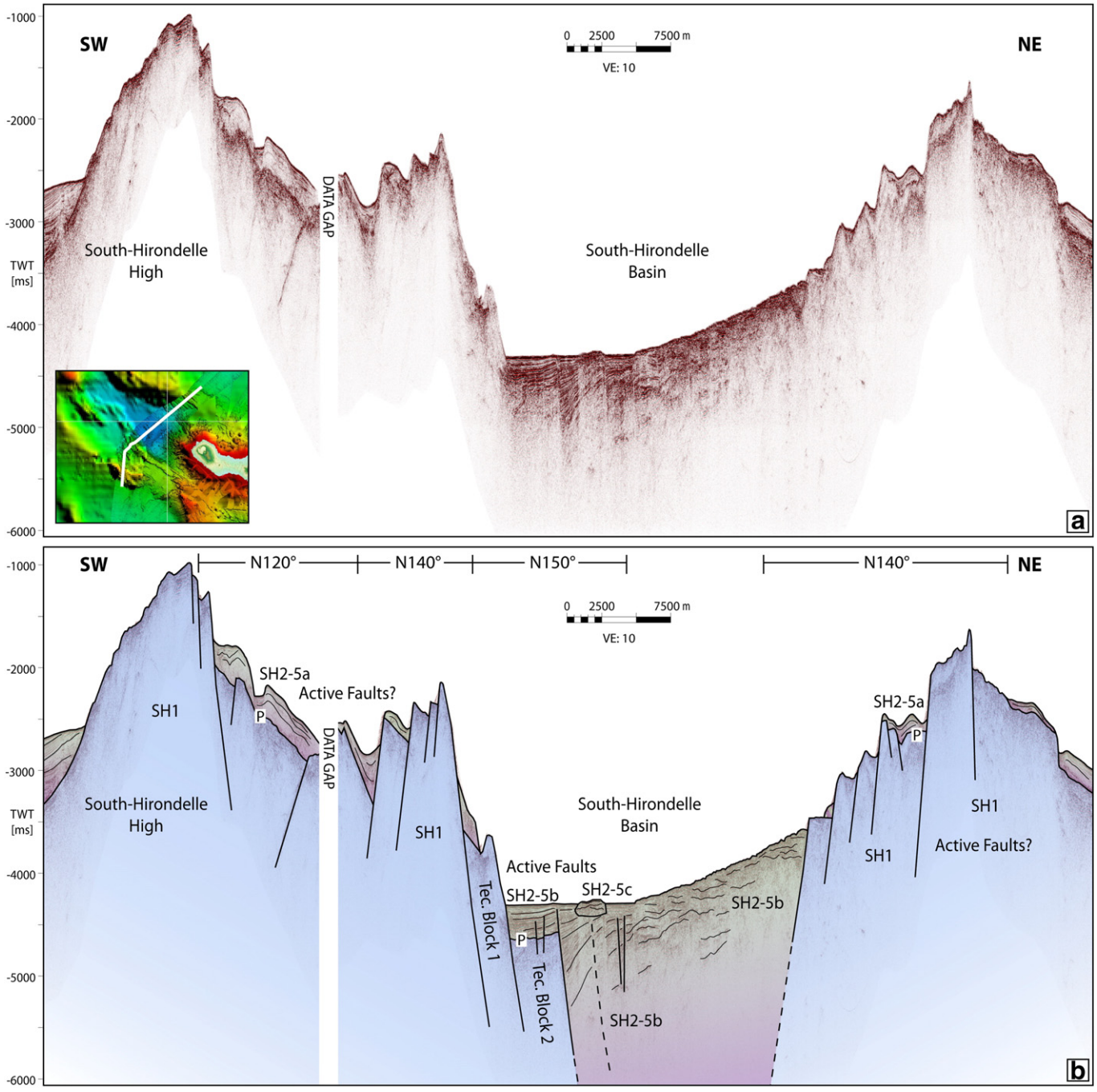

Fig. 4. Seismic section (a) and corresponding interpretation (b) covering the South-Hirondelle Basin and the adjacent volcanic ridges west of São Miguel Island in a SW–NE direction. Dashed line: Inferred fault. VE: Vertical Exaggeration. For the section's location see inset, Figs. 2 or 3.

margin (Fig. 4). The recent activity of the N140° trending faults on top of the northeastern ridge and its southwestern counterpart is ambiguous. Depositional voids can be considered either as current induced moats or as the consequence of recent tectonics. These two processes do not exclude each other, both processes may act simultaneously. Mapped faults within Sete Cidades region (Ferreira, 2000; Queiroz, 1997) trend N140° and represent the onshore continuation of the faults shaping the southern flank of the northeastern ridge (Fig. 3a).

4.2. Monacco Graben & Monacco Bank

4.2.1. Observations bathymetry

The Monacco Graben (MG) separates the island shelf in the north and the Monacco Bank Plateau (Fig. 3a/b). Several predominantly circular cones are located within the graben, most of them in the very southeast where the graben pinches out. The graben flanks are defined by the smooth 10°–15° dipping slope of the island's shelf in the north and a steep flank in the south showing slope angles of up to 70° (marked with A in Fig. 3a).

Monacco Bank (MB) represents a prominent 70 km long bathymetric feature with a maximum width of 25 km (Fig. 5a/b). Being elevated by 1700–2000 m above the surrounding basin floors, its top is characterized by a plateau slightly ascending to the northwest. This plateau forms the southern shoulder of the Monacco Graben (Fig. 3b). A set of normal faults disrupt the western bank from north to south usually characterized by vertical offsets of 50 to 100 m. The scarps mostly dip westwards with 30°–45°. To the east, faulting becomes less obvious.

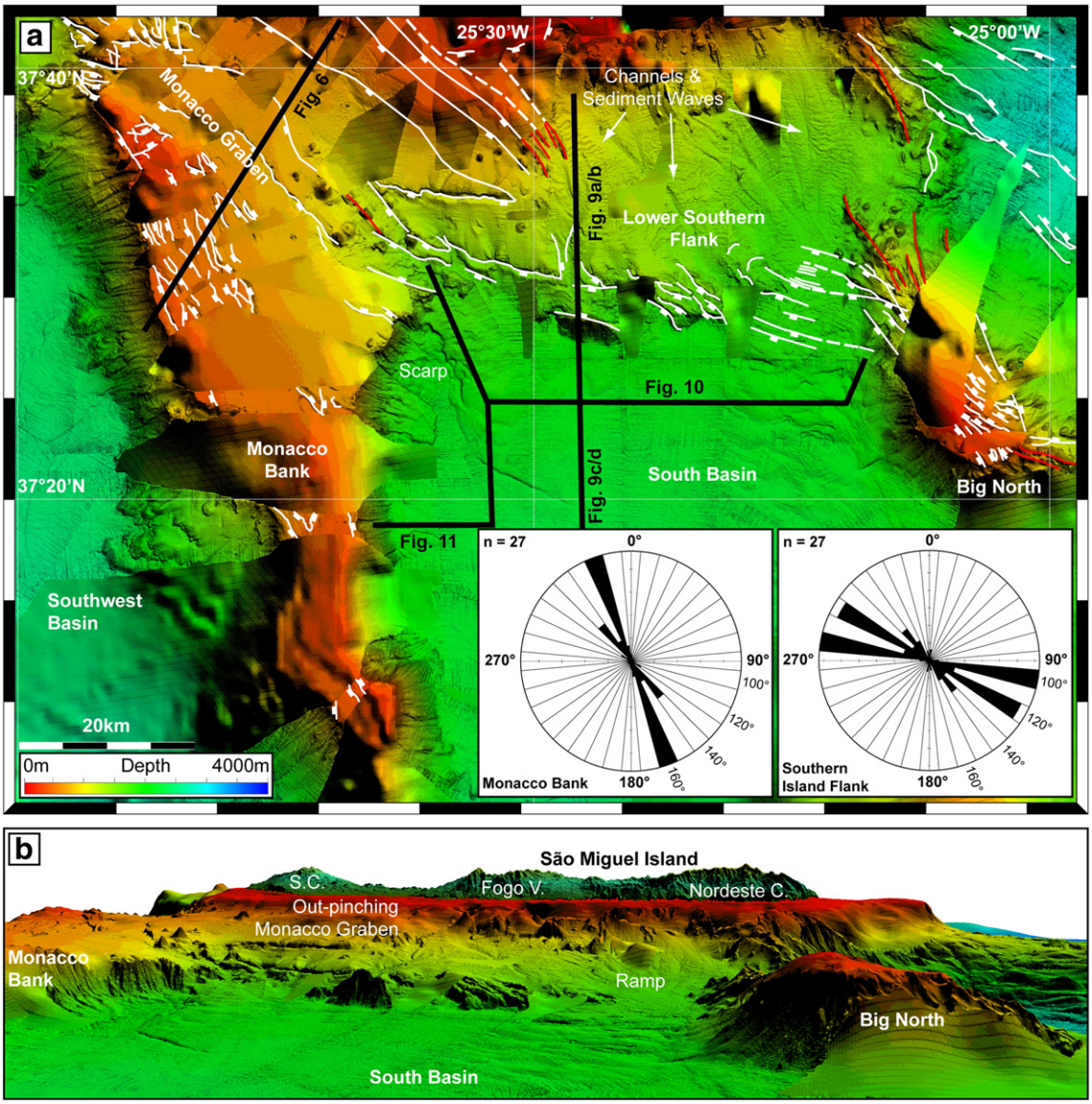

Fig. 5. Bathymetry and picked faults in the southern working area (a) and 3D view (b). White line: Fault. Dashed white line: Inferred fault. Red line: Volcanic lineament. Thick black lines indicate seismic profiles. S.C.: Sete Cidades Volcano. Viewing direction of 3D sight from Santa Maria Island to the north. Illumination from N90° with an azimuth of 60°.

Faults show two orientations: Monacco Graben reveals a clear N120° main trend (see upper right rose diagram in Fig. 3a); and faults on top of Monacco Bank strike N160° similar to Monacco Bank itself (see left rose diagram of Fig. 5a).

4.2.2. Observations seismic

On top of Monacco Bank, sediment cover is thin and seismically not resolvable (Fig. 6). Accordingly, the basal seismic unit MG2 is subcropping here. It is characterized by low penetration and strong reflection amplitudes. Inside Monacco Graben, two seismic units can be determined. Lower unit MG3 shows a variable reflection pattern from sub-parallel to divergent, contorted and tilted. It partly overlies the basement (horizon Q) unconformably with increasing thickness to the north-east. Horizon R marks the transition from (sub-) parallel to divergent and oblique reflection pattern of unit MG4/5 and also correlates with the root of two of the cones mentioned in Section 4.2.1.

4.2.3. Combined interpretation of bathymetric and seismic data

The Monacco Graben forms a N120° trending and northeast tilting half-graben system with a basement sheared by four synthetic normal faults (marked with S in Fig. 3). Its southern rim is a steep antithetic fault, which also acts as boundary between the N120° and N160° fault setting (marked with A in Fig. 3). The faults clearly offset internal stratification, but vanish within unit MG3 indicating that major tectonics ceased during that time (Fig. 6). In the north-east, one synthetic fault transects the seafloor. However, sediments of unit MG4/5 southwest of the fault are neither tilted nor do they show any indications to be dragged (Fig. 6 bottom, inset). Due to the convex shape of MG4/5 north-east of the fault, we rather assume bottom currents to be the reason for non-deposition along the fault plane instead of recent tectonic movements. This is also in accordance with the fact that Monacco Graben shows no recent seismicity (Appendix 1). Hence, we interpret MG4/5 as predominantly current controlled post-tectonic sediments. The tilted and divergent reflection pattern of MG3 reflects growth-strata indicating syn-tectonic sedimentation conditions during graben formation. A northward increasing thickness of unit MG3 (Figs. 6 and 7e) refers to a major sediment source north of the graben, probably indicating strong volcanism in the present-day Sete Cidades region. However, the cones interpreted as to be of volcanic origin (see Mitchell et al. (2012) and Stretch et al. (2006) for comparable structures southeast of Pico Island)

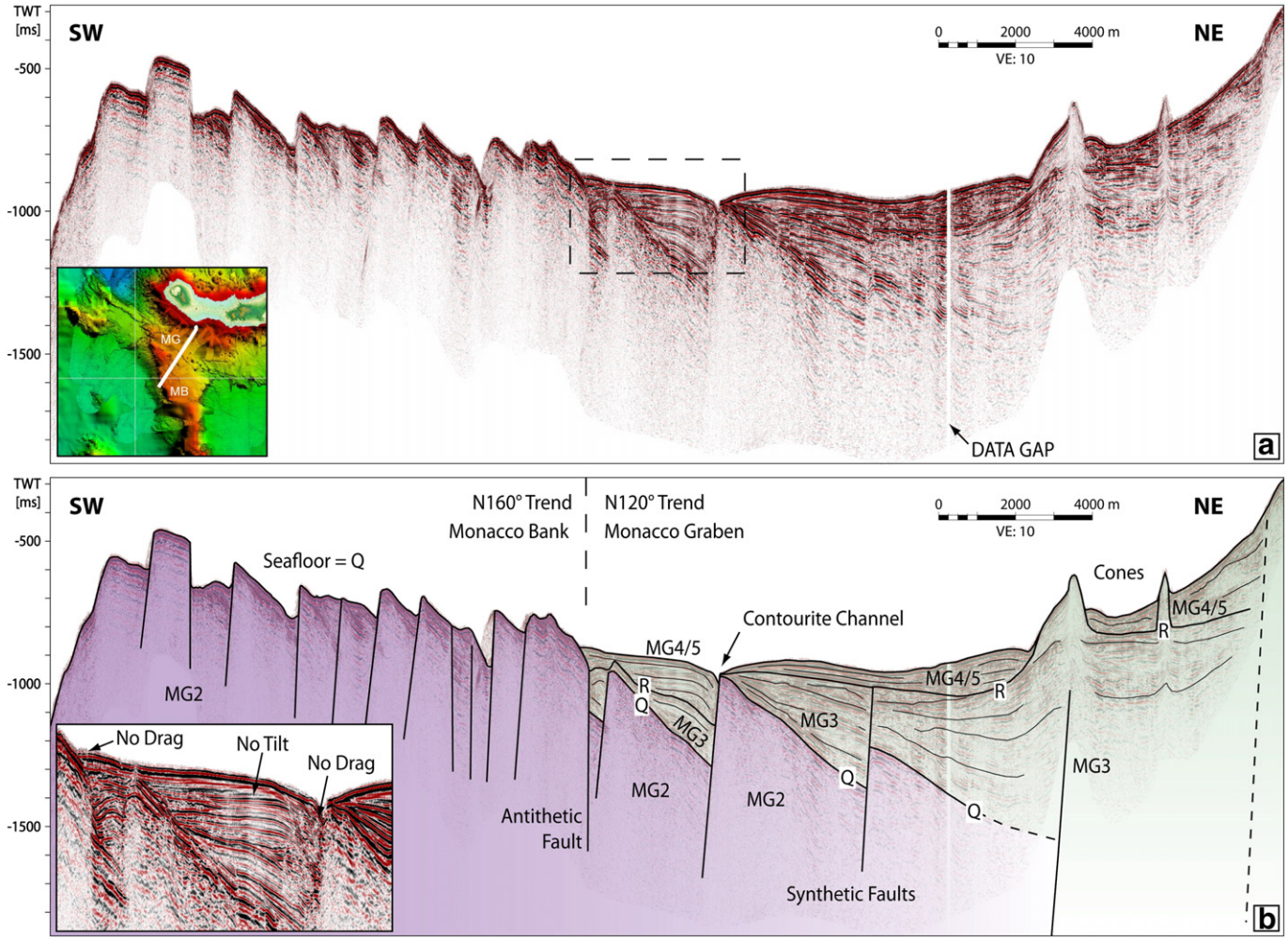

Fig. 6. Seismic section (a) and interpretation (b) covering the Monocco Graben southwest of São Miguel Island. Dashed line: Inferred fault. Dashed black box indicates location of zoomed seismic in (b). MG: Monocco Graben; MB: Monocco Bank. VE: Vertical Exaggeration. For the section's location see inset, Figs. 2, 3 or 5.

show that volcanism also occurred within the graben. Younger MG4/5-sediments onlap the cone flanks (Fig. 6), thus indicating that volcanism stopped at the end of graben formation. Since MG2, interpreted as volcanic basement, is not covered by sediments on top of Monocco Bank, it is not possible to derive any kinematic conditions in time along the N160° trending faults system.

4.3. Southwest Basin

4.3.1. Observations bathymetry

The Southwest Basin (SW) is located southwest of São Miguel Island and is bounded by the South-Hirondelle High in the north and the N160° trending Monocco Bank in the east (Fig. 2). In the southwestern part, an ~N130° oriented volcanic ridge (Southwest Ridge) is observable.

4.3.2. Observations seismic

The basin comprises four seismic units (Fig. 8a–e). Horizon Q traces the continuation of the flank of Monocco Bank and represents the top of unit SW2 (Fig. 8c/e). It shows a strong irregular reflection pattern with low penetration proximal of Monocco Bank and passes over to parallel reflections in the distal domain. Horizons Q and SW2, respectively, onlap the flanks of South-Hirondelle High (horizon P in Fig. 8b) and the Southwest Ridge (SW1 in Fig. 8e). Overlying unit SW3 shows a similar spatial reflection pattern, but reflections appear more regular. It converges towards the east where SW3 merges with the flank of Monocco Bank. Sediment thickness reaches a maximum of up to 420 ms in the northeastern part of the basin (Fig. 7e). Horizon R is the base of unit SW4/5 (Fig. 8b, c, e). It is characterized by a package of low reflection amplitudes at its bottom. Near the bathymetric highs in the north and southwest, it reveals truncated and/or converging to parallel reflections. Further to the east, intercalated packages with mostly chaotic, hummocky or contorted reflections are observable (Fig. 8a, marked in yellow in Fig. 8e) and the overall reflection pattern becomes more irregular. Thickness increases to the south, where it reaches maximum values of more than 500 ms (Fig. 8a).

4.3.3. Combined interpretation of bathymetric and seismic data

The high amplitudes and highly irregular reflections of SW2 terminating within the flank of Monocco Bank (no onlap) identify this unit as being generated and deposited during the volcanic development of Monocco Bank (Fig. 8c/e). This also applies to SW3, as the unit converges towards the flank of Monocco Bank as well, but due to the more regular reflections we suggest that this unit rather represents erosional products than in-situ generated volcanic material. Thickness distribution (Fig. 7e) and geometry (Fig. 8c) indicate the bathymetric high between the South-Hirondelle High and Monocco Bank as major sediment source. Distal of the Monocco Bank, sedimentation became more uniform, which is also reflected by the parallel reflection pattern in the western basin (Fig. 8a, b, d). SW2 and SW3 both onlap the flanks of the South-Hirondelle High (Fig. 8b) and the N130° trending Southwest Ridge (Fig. 8d/e) highlighting that the N160° trending Monocco Bank must be geologically younger.

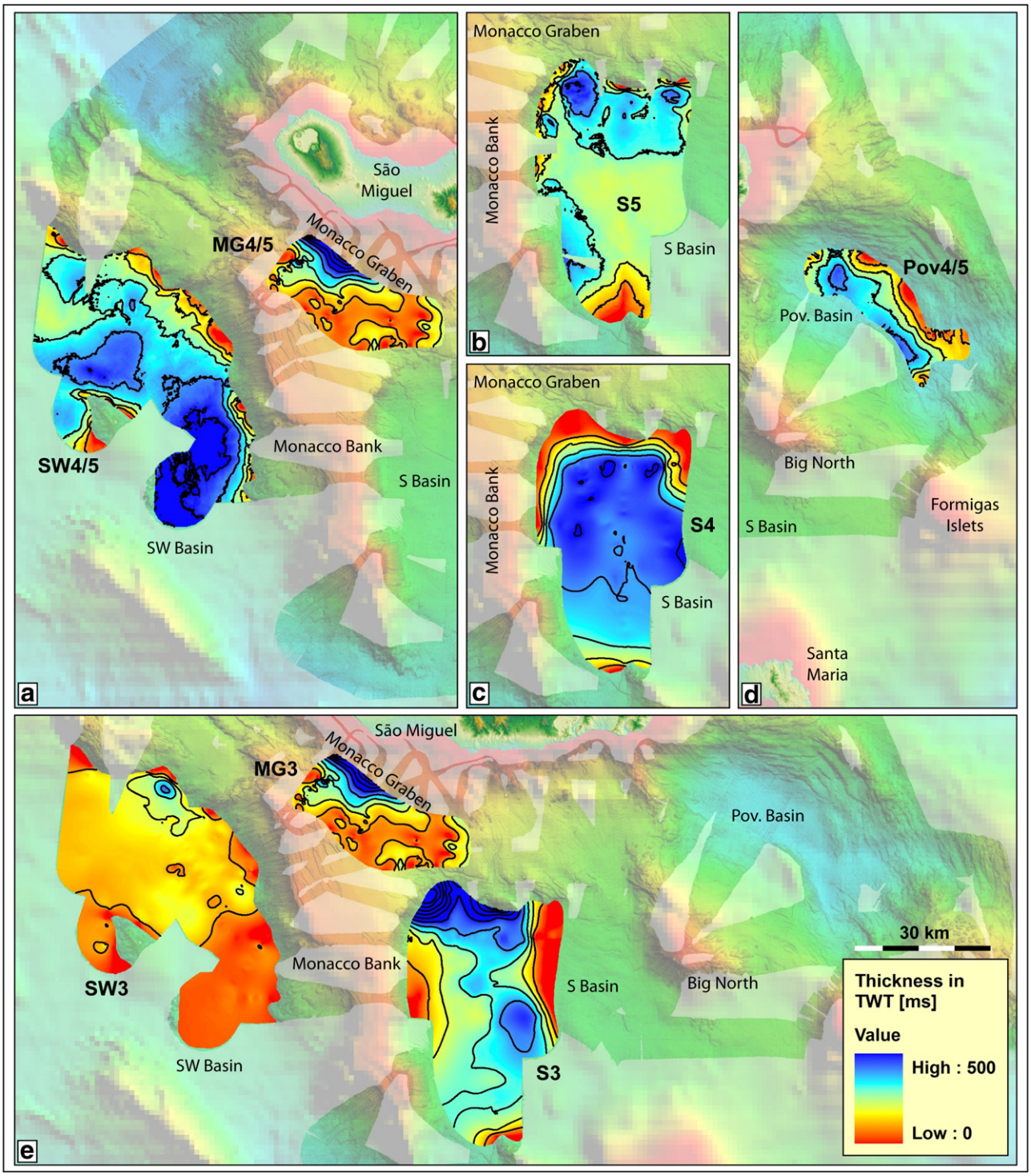

Fig. 7. Thickness of seismic units as defined in the text. (a) Units SW4/5 and MG4/5; (b) unit S5; (c) unit S4; (d) unit Pov4/5; (e) units SW3, MG3 and S3. Scale is in ms, isopachs every 100 ms (corresponds to m, if an interval velocity of 2000 m/s in the sediments is assumed). Upward alignment of sub-figures corresponds to the chronology of their deposition. See also Table 1.

After the evolution of Monacco Bank, uniform sedimentation in the basin resulted in the parallel stratified reflection pattern of SW4/5 (Fig. 8a/e). In contrast, disrupted and irregular reflections at the northeastern basin margin indicate mass transports. The intercalated packages with chaotic and contorted reflection patterns (Fig. 8a, marked in yellow in Fig. 8e) reflect the associated rough and blocky deposits (Bull et al., 2009).

4.4. Lower southern flank of São Miguel & South Basin

4.4.1. Observations bathymetry

The submarine domain south of São Miguel consists of the island's flank and the South Basin (Fig. 5a). The flank is characterized by the out-pinching Monacco Graben in its western part and by a ramp of ~500 km^2 dipping basinward with 2° to 3° in its eastern part (Fig. 5b).

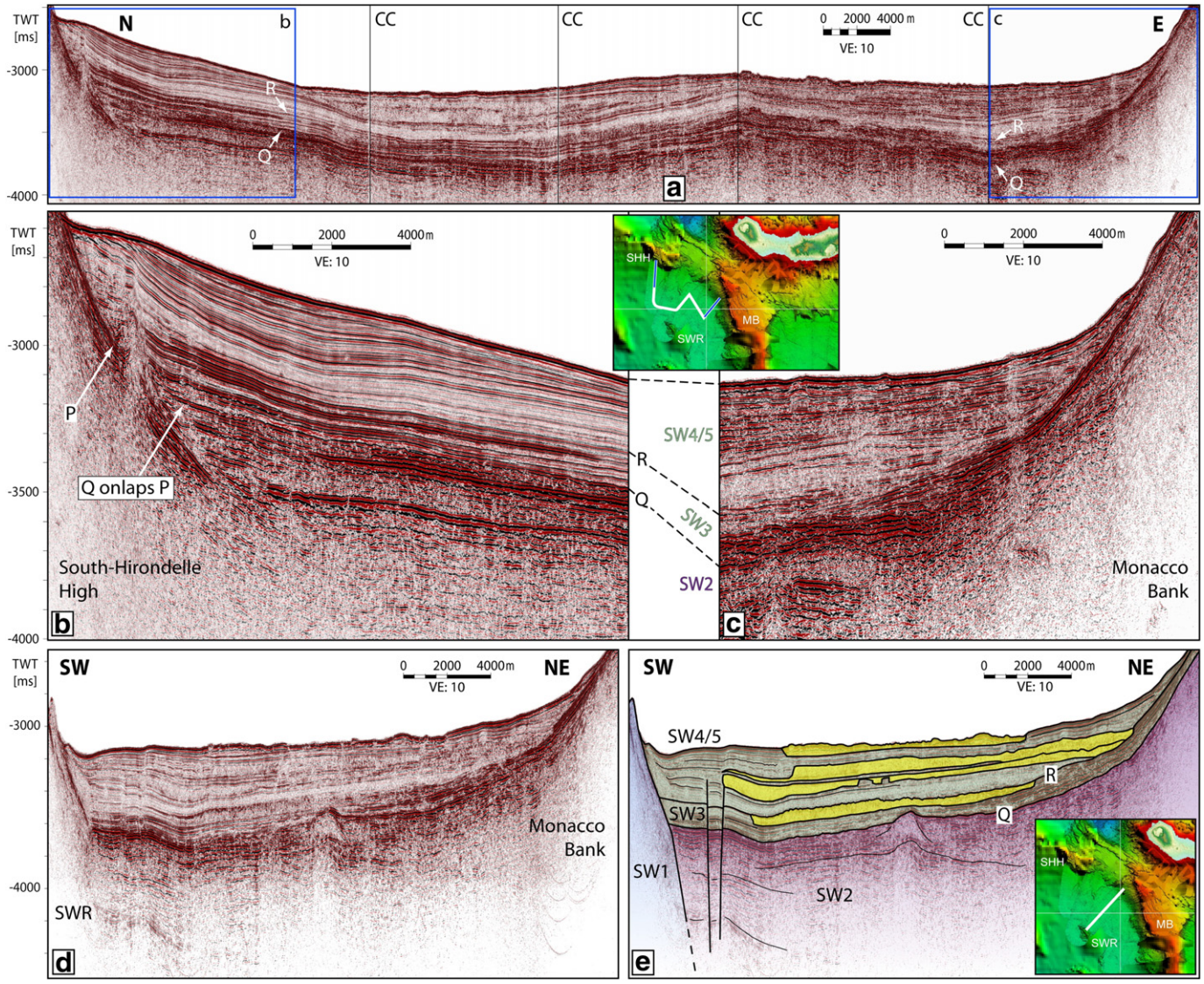

Fig. 8. Seismic sections in the basin southwest of São Miguel Island. (a) Composite plot connecting the South-Hirondelle High (SHH) and Monacco Bank (MB). It shows that the flank of MB in (c) and horizon Q, respectively, onlaps the SHH in (b). SW–NE oriented seismic line (d) and its interpretation (e). Note the onlap configuration of horizon Q at the Southwestern Ridge (SWR). Yellow color indicates mass transport deposits. VE: Vertical Exaggeration. For the section's location see inset or Fig. 2. Vertical black lines indicate course changes (CC).

The South Basin (S) shows water depths ranging from 1800 m in the northwest to 2300 m in the south. It is bordered by the Monacco Bank in the west, by the Big North High in the east and by the N140° trending South Ridge (SR)/Santa Maria Island in the south (Fig. 2). Both regions are separated by a set of faults and tilted blocks.

These faults reveal a strong Monacco Graben related N120° trending component in the west. In the east, faults trend N100°. They mainly dip to the south terminating at the northwestern flank of the Big North High.

4.4.2. Observations seismics

Seismic penetration at the lower flank of São Miguel is low and a sub-division in multiple stratigraphic units is not possible (Fig. 9a/b). The reflection pattern shows high amplitudes and distorted reflections. Downslope, northward dipping reflections are observable before the flank terminates at a bathymetric high, which reveals weak internal stratification parallel to its southern slope.

In contrast, the sedimentary infill of the South Basin can be separated into six seismic units. The lowermost units S1a (Fig. 9c/d) and S1b (Fig. 10) are both characterized by limited penetration, chaotic reflections and high amplitudes at the top. Unit S2 is poorly imaged, at least a weak internal stratification can be traced (Figs. 9c/d and 10). In the west, top of S2 (horizon Q) merges with the flank of Monacco Bank (Fig. 11). Overlying unit S3 shows a sub-parallel stratification, which terminates in an onlap configuration against S2 (Fig. 11), S1a (Fig. 9) and S1b (Fig. 10) in the west, south and east, respectively. Top of S3 (horizon R) is defined by the northwestern basin flank where Monacco Graben pinches out (Figs. 10/11). Here, S3 shows its maximum thickness (Fig. 7e) and internal reflections downlap on horizon Q (Fig. 10). In the basin, S3 is concordantly overlain by the well stratified seismic unit S4, showing a constant thickness of approximately 450 ms (Fig. 8c). S4 onlaps S1a in the south (Fig. 9c/d) and terminates vertically against a package of disrupted, contorted and tilted reflections onlapping S3 in the northwest. In the east, S4 terminates vertically against or onlaps a package of chaotic/distorted reflections covering unit S1b (see large yellow areas on top of horizon R in Fig. 10). However, the western base of this package is hardly detectable, but is possibly coinciding with horizon R. In the basin center, uppermost seismic unit S5 reveals a parallel reflection pattern and overlies unit S4 concordantly (Figs. 9c/d and 10). In the south reflections converge, onlap the tilted part of unit S4 and the unit pinches out (Fig. 9c/d).

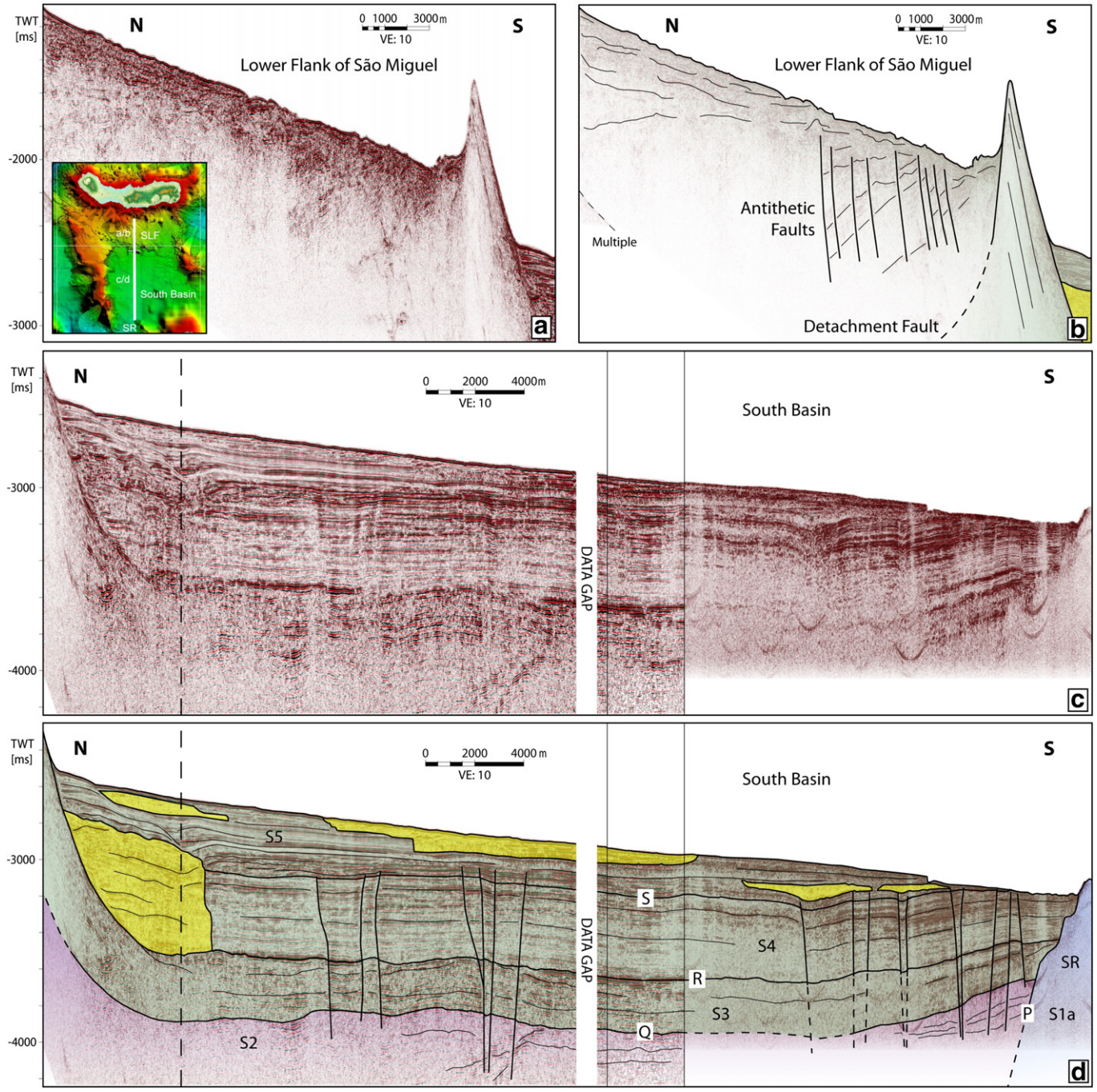

Fig. 9. Seismic sections and corresponding interpretations covering the southern slope of São Miguel Island (a, b) and the South Basin (c, d) in a N–S direction. Yellow color indicates mass transport deposits. SLF: Southern lower flank of São Miguel; SR: South Ridge. VE: Vertical Exaggeration. For the section's location see inset, Figs. 2 or 5. Vertical dashed line marks intersection with the W–E directed profile (Fig. 10). Vertical black lines indicate intersection of profiles.

At the northwestern and eastern basin margins, reflection pattern changes to a contorted and/or lenticular facies (Fig. 10). Several packages of mostly chaotic and/or contorted reflections are embedded in or overlain by S5 (marked with yellow in Figs. 9d, 10b and 11b). Close to the eastern package showing a chaotic reflection pattern, reflections of S5 get more irregular (Fig. 10b). A set of faults are traceable in the basin, most of them terminating at the base of or inside unit S5. Faults piercing the seafloor are not observable.

4.4.3. Combined interpretation of bathymetric and seismic data

Due to the poor penetration of S1a and S1b, these units are interpreted as magmatic basement, which has been erupted/deposited during the evolution of the South Ridge beside Santa Maria Island and Big North High, respectively (Figs. 9c/d and 10). In both cases, the poorly resolved internal stratification of S2 terminates against S1a/b. Therefore, we interpret that horizon Q (which is the stratigraphic continuation of the flank of Monacco Bank and top of S2) onlaps horizon P (which is the top of the magmatic basement). This implies that Monacco Bank is geologically younger than these corresponding structures. The onlap configuration of horizon R (which is the stratigraphic continuation of the northwestern basin margin flank and the out pinching Monacco Graben, respectively) at the flank of Monacco Bank (horizon Q, Fig. 11) shows that unit S3 was deposited after the formation of Monacco Bank but during the formation of Monacco Graben. The southern flank of the

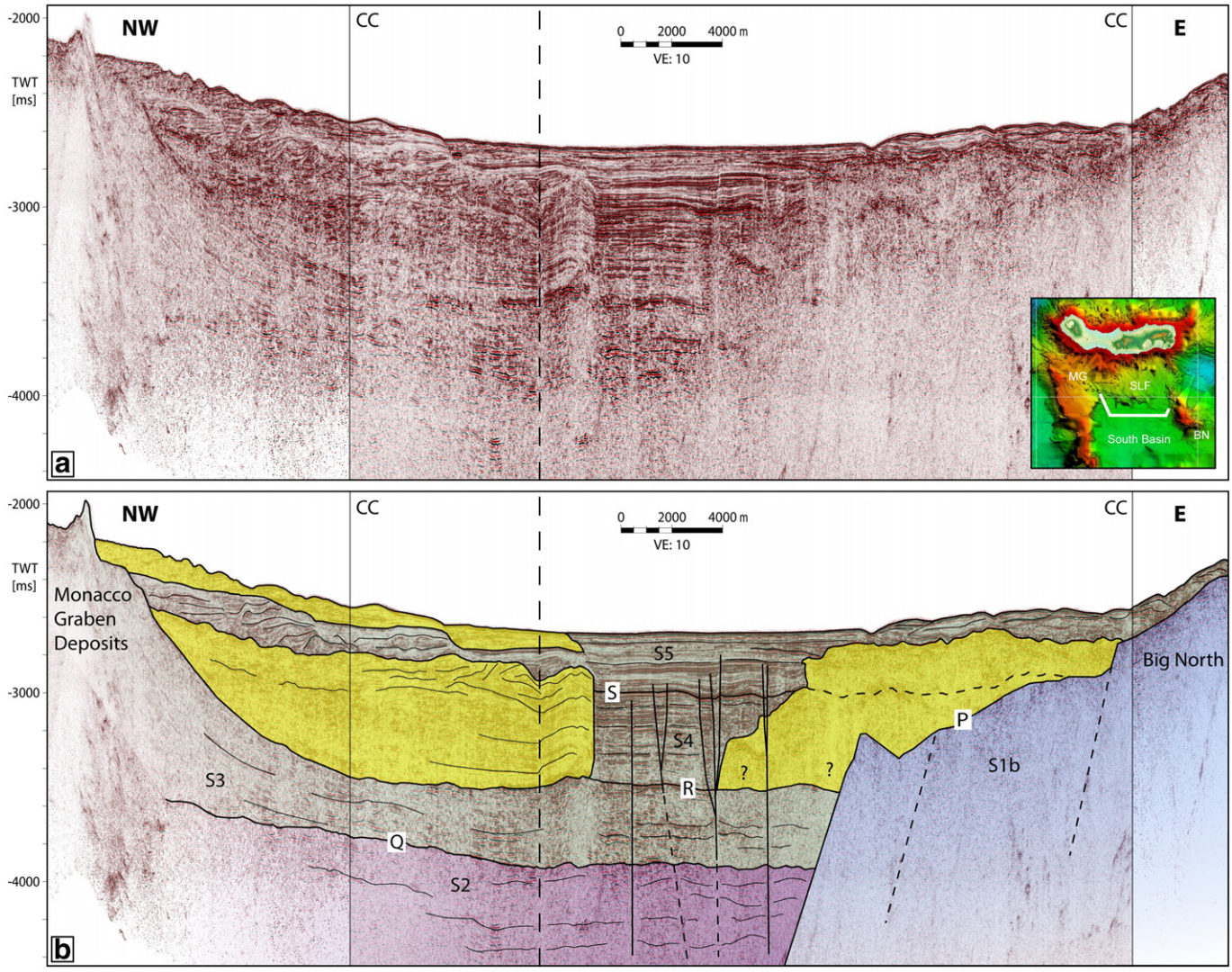

Fig. 10. Seismic section (a) and interpretation (b) covering the South Basin in a W–E direction. Yellow color indicates mass transport deposits. SLF: Southern lower flank of São Miguel; MG: Monacco Graben; BN: Big North. VE: Vertical Exaggeration. For the section's location see inset, Figs. 2 or 5. Dashed line marks intersection with the N–S directed profile (Fig. 9). Vertical black lines indicate course changes (CC).

tilted block separating the lower flank of São Miguel and the South Basin (Fig. 9a/b) is built up by unit S3 (Fig. 9c/d). For this reason, we conclude that the evolution of the block and the adjacent fault system (Fig. 5) is linked to the formation of Monacco Graben. Thus, the faults north of the block (Fig. 9a/b) could be antithetic branch faults of a north facing detachment fault. After the formation of Monacco Graben, the well stratified unit S4 was deposited in the basin (e.g. Fig. 9c/d). Since thickness of unit S4 is constant and faults are neither characterized by an upward increasing offset of internal reflections nor terminating within the unit, sedimentation occurred during isotropic sedimentation conditions and tectonic quiescence. After S4 times, tectonics initiated faulting and tilting of the basin sediments (Fig. 9c/d). Due to the fact that faults crop out within S5 and local vertical movements are compensated by S5 sediments, tectonic activity in the basin is interpreted as being limited to early S5 times only. Additionally, maximum thickness (Fig. 7b) and the contorted/lenticular reflection pattern of unit S5 in the northwestern and eastern part of the basin (Fig. 10) indicate an anisotropic, southward directed sediment transport coming from São Miguel Island. The packages characterized by a chaotic/contorted reflection pattern are again interpreted as mass transport deposits (yellow areas in Figs. 9d, 10b and 11b). The huge deposit in the eastern basin represents a special case (Fig. 10b). Since S4 reflections onlap the lower part of the body and S5 reflections are slightly irregular close to the upper part of the body, it is likely that it was generated by several events during S4 and S5 times. Other mass transport deposits can be dated to S5 times, since they are embedded in S5 sediments (e.g. Fig. 9d) or since the remobilized material includes S5 sediments (Fig. 10b, at the western termination of horizon S). Possible trigger mechanisms could be gravitational load or tectonic events or a superposition of both effects.

4.5. Povoação Basin & Big North High

4.5.1. Observations bathymetry

The Povoação Basin (Pov) links São Miguel Island and East Formigas High, a shoal with a minimum water depth of 100 m and covered with many cones (Fig. 12a/b) similar to those observed in the Monacco Graben (Fig. 3a). The basin is characterized by a water depth of 2930 m in its center and its conspicuous curved shape. Similar to the South-Hirondelle Basin, the northeastern margin is crosscut by a large number of mostly basinward dipping normal faults occasionally forming

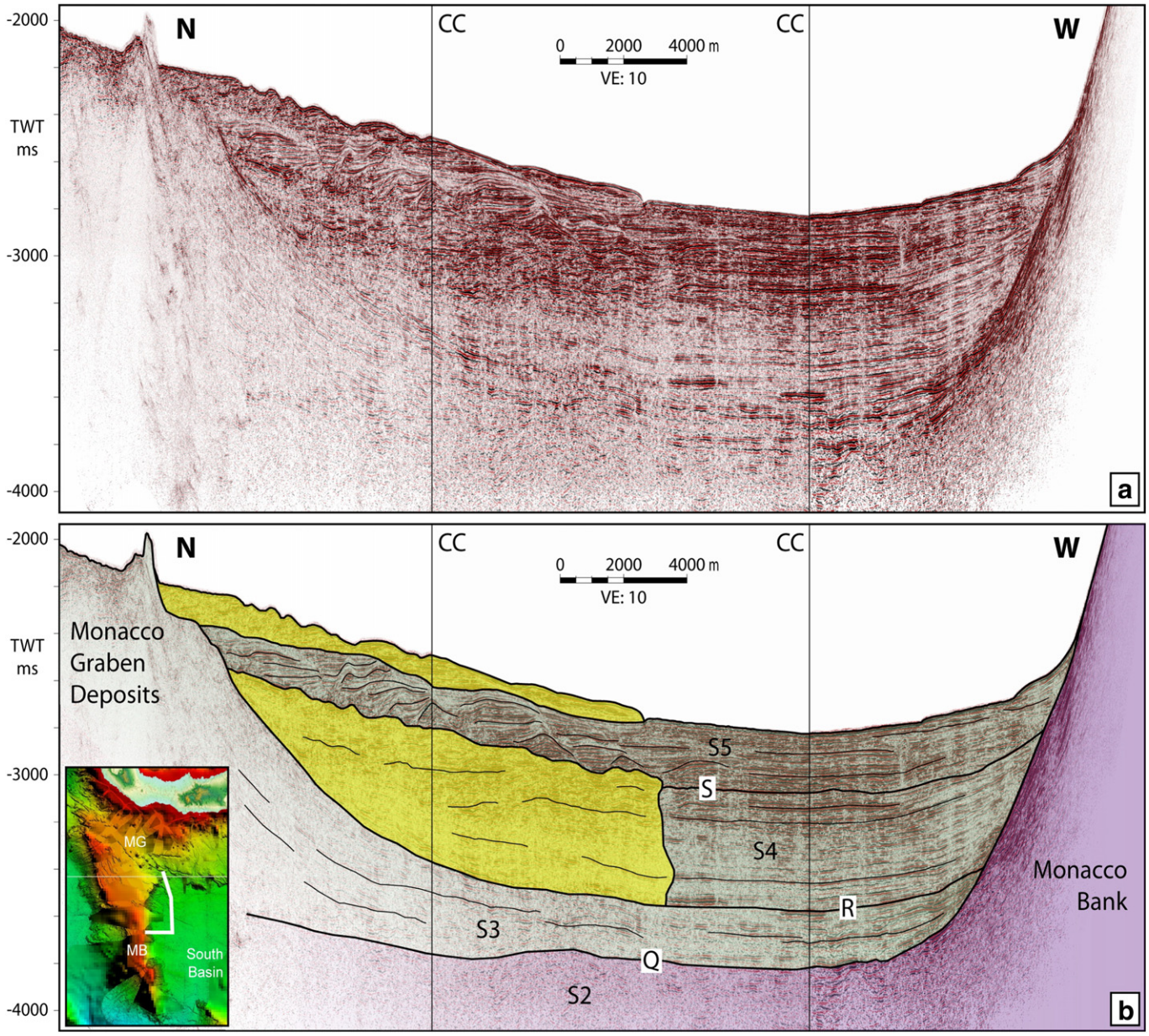

Fig. 11. Seismic section (a) and interpretation (b) showing the temporal relationship of Monacco Graben and Monacco Bank. Yellow color indicates mass transport deposits. MG: Monacco Graben; MB: Monacco Bank. VE: Vertical Exaggeration. For the section's location see inset, Figs. 2 or 5. Vertical black lines indicate course changes (CC).

small ancillary basins, whereas the southwestern margin is dominated by three fault scarps also dipping basinwards (marked as MF in Fig. 12a–c) — one forming the northeastern slope of Big North High, another between Big North and the basin and a further one representing the transition from the margin to the flat basin. To the south, they split up in a set of normal faults (SF in Fig. 12a/b). Scarps usually exhibit dip angles of 30° to 40° on both sides. Vertical offsets normally range from 100 m to 300 m at the northeastern margin, but vary up to 700 m at the southwestern one. South of East Formigas High and in prolongation of the northeastern basin margin two dominant fault scarps are observable. They show the same dip direction and similar dip angles, but their vertical offsets reach values of up to 1000 m (marked as DF in Fig. 12a).

Southwest of the Povoação Basin, Big North High shows a flat top (Fig. 12a) with an average water depth of ~250 m strongly offset by mainly northeast dipping fault scarps (30° to 60°, vertical offsets of 50 m to 100 m).

The dominant strike direction on top of Big North and along the southwestern basin margin is N130° to N140° (lower left rose diagram in Fig. 12a). Volcanic lineaments north of Big North and two of the major normal faults (faults marked with yellow MF in Figs. 12 and 13) reveal a N160° trend. In contrast, the northeastern basin margin can be divided into three zones of strike directions. North of the basin and close to São Miguel Island, a clear N90° to N110° trend is evident. In the northeast, a set of faults are oriented N130° to N140°. Faults and lineaments east of the basin as well as southeast of East Formigas High are strongly dominated by a N160° trend (A, B, C/DF, respectively, and upper right rose diagram in Fig. 12a).

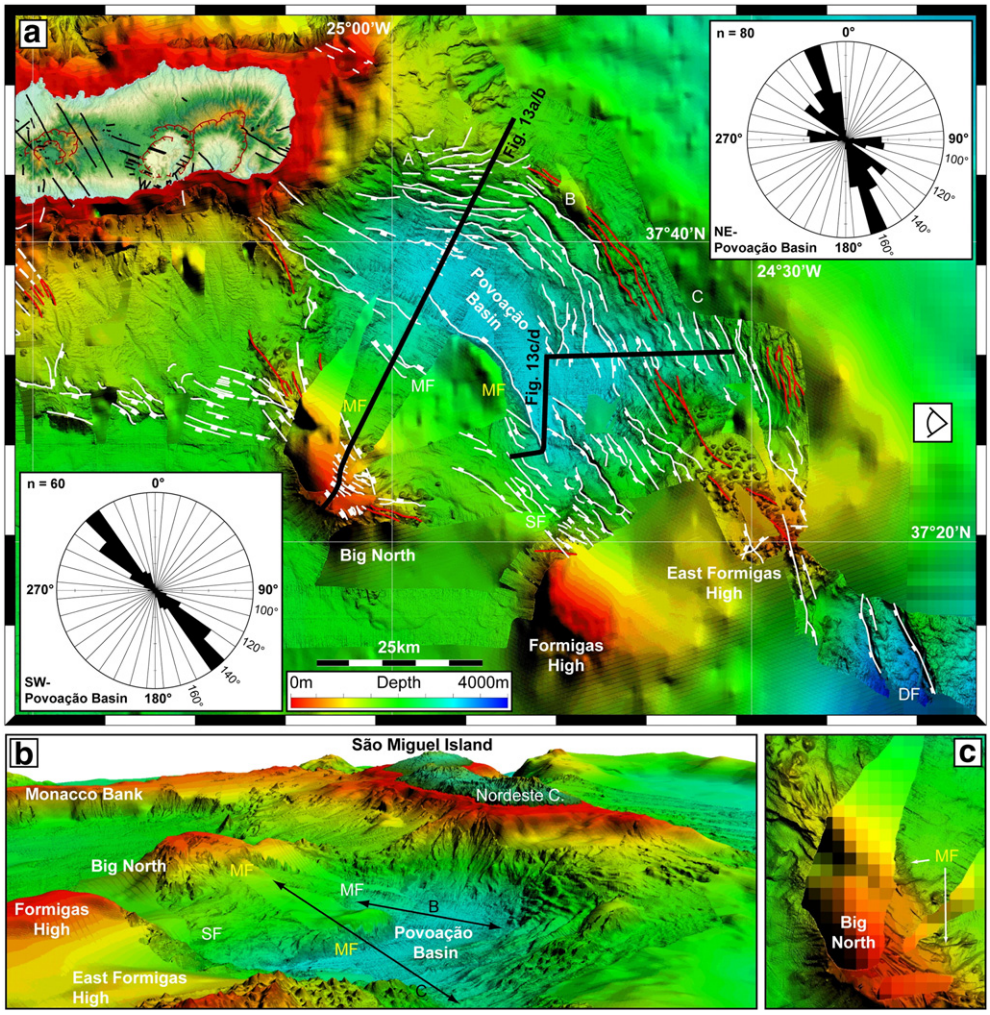

Fig. 12. Bathymetry and picked faults in the eastern working area (a), 3D view (b) and zoom of Big North High (c). The northeastern basin margin shows three zones of strike directions: N90° to N110° (A), N130° to N140° (B), and N160° (C). Two dominant faults south-east of East Formigas High strike N160° as well (DF). Three major faults are present at the southwestern margin trending N140° (MF, white) and N160° (MF, yellow). To the south these three fault planes split up in a set of normal faults (SF). White line: Fault. Dashed white line: Inferred fault. Red line: Volcanic lineament. Thick black lines indicate seismic profiles. Eye symbol denotes the viewing direction of the bottom 3D sight. Illumination from N90° with an azimuth of 60°. Onshore faults based on Carmo (2004), Carvalho et al. (2006) and Guest et al. (1999).

4.5.2. Observations seismics

Seismic penetration at the basin margins is again very low and the corresponding acoustic basement (Pov1) is characterized by chaotic reflections with high amplitudes (Fig. 13). While stratified sediments of unit Pov2/3 concordantly overlie the tilted acoustic basement (Pov1) within the ancillary basin, they discordantly cover unit Pov1 within the main basin. Reflections are usually parallel and tilted but slightly divergent in the inner part of the ancillary basin (Fig. 13c/d). Sediments of the uppermost seismic unit Pov4/5 onlap both top Pov1 (horizon P) and top Pov2/3 (horizon R). Pov4/5 is mostly characterized by divergent reflections, but on top of the southwestern margin an oblique subparallel to lenticular reflection pattern dominates (Fig. 13a/b). Unit Pov4/5 thickens to 150 ms within the ancillary basin and to 450 ms in the main basin (Fig. 7d).

4.5.3. Combined interpretation of bathymetric and seismic data

Due to the seismic characteristics of the unit, we interpret Pov1 to be the magmatic basement, which developed during the evolution of Big North High and the present-day northeastern basin margin. Mostly parallel stratified sediments of unit Pov2/3 filling up accommodation space which had been created by faulting of the magmatic basement (Fig. 13b/d), indicate 1) extension of the basement during Pov1 times, and 2) post-tectonic sedimentation during Pov2/3 times (divergent reflections indicate syn-tectonic sedimentation in a small part of the ancillary basin and the northern Povoação Basin only).

East of the basin, N160° trending normal faults offsetting and tilting the seafloor as well as the parallel Pov2/3 sediments (Fig. 13d and marked with C in Fig. 12a) denote these faults to be active from the beginning of Pov4/5 times until now. On top of Big North High, N130°/N140° faults, terminating eastwards against the N160° oriented fault scarp (marked with yellow MF in Figs. 12a, c/13b), lead to the suggestion that this scarp is younger than the faults on top. Additionally, diverging reflections of Pov4/5 in the southern basin (Fig. 13d) show active subsidence along the N160° trending fault (yellow MF in Fig. 13d). Extension could also be partly accommodated at the N140° oriented normal fault west of the N160°-fault (white MF in Fig. 13d). However, the northwestern continuation of the N140°-fault (white MF in Fig. 12a) seems not to be active, since uppermost unit Pov4/5 shows no evidence of syn-tectonic sedimentation (white MF in Fig. 13b).

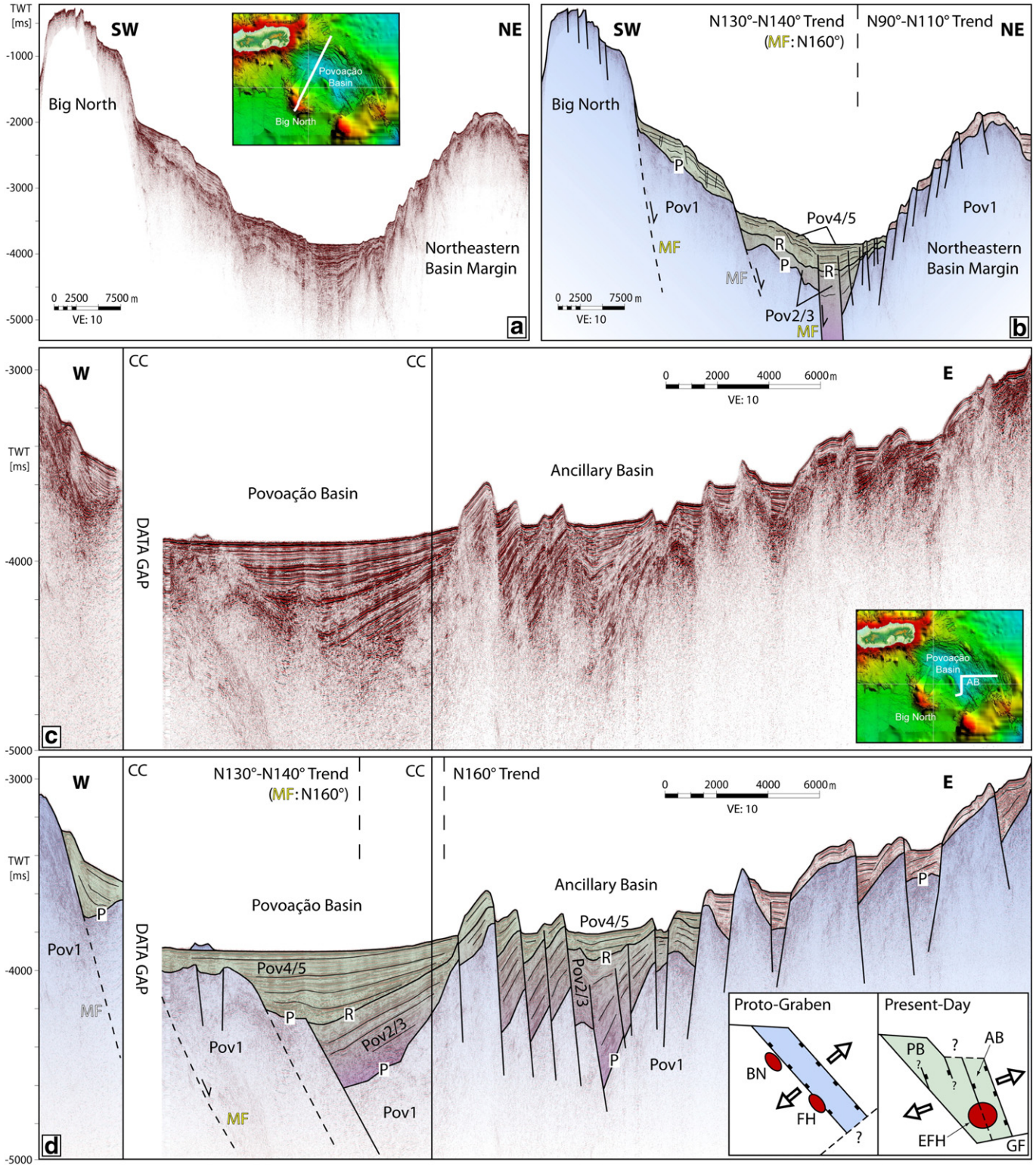

Fig. 13. Seismic sections and corresponding interpretations covering the Povoação Basin (PB) south-east of São Miguel Island. One seismic line crosses the northern part of the basin in SW–NE direction (a, b), another one the southern part and the ancillary basin (AB) in an overall W–E direction (c, d). MF marks major fault planes trending N130°–N140° (white) and N160° (yellow). Dashed line: Inferred faults. VE: Vertical Exaggeration. For the section's location see insets, Figs. 2 or 12. Vertical black lines indicate course changes (CC).

Therefore, we assume that the Povoação Basin was formed in two phases (see sketch in Fig. 13d). First, a N130°–N140° trending (proto-) graben developed during Pov1 times. Corresponding N130°–N140° trending faults can be observed across the southwestern margin and on top of Big North High. Faults with the same orientation at the north-eastern margin are less dominant but can also be found northeast of the central basin (marked with B in Fig. 12a). After a time of reduced extension (Pov2/3), horizon R marks the onset of the second phase (Pov4/5,

Fig. 13), which is active until today. Extension is mainly accommodated along N160° trending faults and focuses on the southern and the ancillary basin (marked with C in Fig. 12a). In the northern part of the basin, less distinct tilted reflections of Pov4/5 within the basin (Fig. 13b) possibly indicate that tectonics in this area are more dominated by transfer than slip movements.

4.6. Summary of observations

Based on the presented bathymetric and seismic data, we can finally summarize some major results:

1. Strike directions of faults and structural lineaments group into three major categories. Northwest of São Miguel Island, a N140° trend with intercalated N150° trending structures is observable (Fig. 3a; marked with red and dark blue in Appendix 2, respectively). The N140° trend is also present southeast of the island, in particular at the southwestern margin of the Povoação Basin and on top of Big North High (Fig. 12a). The eastern margin of the Povoação Basin and the East Formigas High is clearly dominated by a N160° trend (Fig. 12a; marked with gray in Appendix 2). This trend is also reflected by Monacco Bank and its fault system on top (Fig. 5a). In between these two settings, structures mainly strike N90° to N110° (Figs. 5a and 12a; marked with light blue in Appendix 2) or reflect the Monacco Graben trend of N120° (Fig. 3a; marked with green in Appendix 2).
2. The N160° trending Monacco Bank postdates the evolution of the South-Hirondelle High, the Southwest Ridge, the South Ridge west of Santa Maria Island and the Big North High, all approximately oriented N140°.
3. The Monacco Graben is younger than the Monacco Bank.
4. The Monacco Graben shows no major recent tectonic activity.
5. Since the evolution of Monacco Graben, the South Basin first underwent a tectonically inactive period with uniform sedimentation conditions, followed by a period associated with an N–S directed sediment transport. The transition phase between these periods is characterized by active tectonics.
6. The Povoação Basin evolved in three steps: 1) formation of a N130° to N140° trending proto-basin, 2) sedimentation during reduced tectonics, and 3) syn-kinematic sedimentation during a second tectonically active period with distinct extension along N160° trending normal faults. This period is lasting until today.
7. Volcanic cones and several mass waste deposits are observable (these will be addressed in a later publication).

5. Discussion

5.1. Relative chronostratigraphy

Within the South Basin and Southwest Basin, sediments deposited prior to or during the evolution of Monacco Bank are separated by horizon Q from younger sediments (Figs. 8–11). Horizon Q coincides with the top of the acoustic basement on top of Monacco Bank and the stratigraphic continuation of its flanks. Pre/Syn-Monacco-Bank sediments (represented by the purple units numbered “2” in Figs. 8–11 and Table 1) onlap the magmatic roots of the South-Hirondelle High (Fig. 8b/c), the Southwest Ridge (blue unit SW1 in Fig. 8e), the South Ridge (blue unit S1a in Fig. 9d) and the Big North High (blue unit S1b in Fig. 10b). Units numbered “1” are therefore representing the time of these structures' evolution. S2 and SW2 are postdating this period and predating the end of Monacco Bank formation.

Monacco Bank and Monacco Graben are characterized by a strongly sheared and offset acoustic basement (Fig. 6). Since volcanism did not overprint the faults, we can assume that first Monacco Bank evolved during MG2 times (purple unit in Fig. 6b). Afterwards, its northern part was rifted and Monacco Graben was formed. Lowermost unit MG3 in the graben (Fig. 6b) therefore represents early Post-Monacco-Bank sediments (green colored units in Figs. 6 and 8–10) syntectonically deposited during graben formation. In the Southwest Basin, reflection pattern (Fig. 8) and thickness distribution (Fig. 7e) of the lowermost Post-Monacco-Bank unit SW3 identify the northeastern basin margin between South-Hirondelle-High and Monacco Bank as major sediment source, where the elevated Monacco Graben's northwestern continuation is located. Top of lowermost Post-Monacco-Bank unit S3 in the South Basin is defined by horizon R — the stratigraphic continuation of the northwestern basin margin (Fig. 11b), where S3 shows its maximum thickness (Fig. 8e). Hence, it was deposited after the evolution of Monacco Bank but during the formation of the northwestern basin margin, which is the out-pinching elevated Monacco-Graben. We therefore assume that units MG3, SW3 and S3 altogether reflect the time of Monacco Graben formation.

In the Monacco Graben and Southwest Basin, these units are overlain by unit MG4/5 (Fig. 6b) and SW4/5 (Fig. 8b/e), both reflecting present-day sedimentation conditions. In contrast, the synchronously deposited sediments in the South Basin can be sub-divided into two units: one characterized by homogeneous sedimentation and tectonic quiescence (S4) and a second one (S5) caused by early tectonics and a high sediment flux from the north lasting until today (Figs. 9–11).

Low extension rates during Pov2/3 times in the Povoação Basin (Fig. 13) indicate either a general phase of reduced extension along the Terceira Rift or that extension was mainly accommodated elsewhere. Since there is no evidence for higher and lower extension rates in the sedimentary infill of the South-Hirondelle Basin (Fig. 4), we suggest a region between the South-Hirondelle Basin and the Povoação Basin which accommodated stress during that time. Three regions come into consideration: 1) the area of present-day São Miguel Island, which is too far north, 2) the South Basin, which in fact underwent tectonic stress in the past but with insignificant extension only (Figs. 9 and 10), and 3) the Monacco Bank and Monacco Graben region. Both are indicating distinct extension, since tectonic stress generates pathways for magma ascent and initiates rifting, respectively. Therefore, we chronologically correlate Pov2/3 with the time of Monacco Bank and Graben evolution. Accordingly, syn-tectonic unit Pov4/5 is the temporal equivalent of MG4/5, SW4/5 and S4/S5 in the Povoação Basin, where extension accommodates again after the formation of Monacco Bank and Graben had ended.

5.2. Evolution of the southeastern Terceira Rift

Structures consisting of the earliest units numbered “1” (marked with blue in Figs. 4, 8–11 and 13; see also Table 1) either predominantly reveal a N140° trend (e.g. Southwest Ridge, see Appendix 2) or are overprinted by faults with an equivalent orientation (e.g. Big North High, see Fig. 5). Additionally, it was shown that the Povoação Basin initially evolved along N130°–N140° normal faults (see Section 4.5.3). For these reasons, we suggest that the Azores Plate Boundary here primarily developed within a N40°–N50° extensional regime, which is reflected by N140° trending structures of the southeastern Terceira Rift (Stage I, Fig. 14). Following Neves et al. (2013), the ridges southwest of the Terceira Rift (Fig. 1/Appendix 2) result from volcanism along fissures synchronous with the Rift evolution. Most of them reveal a N140° trend indicating a time of N50° extension as well, since fissures open perpendicular to the minimum stress axis and do not sustain shear. Furthermore, an early direction of extension of N50° was proved based on an analysis of a high resolution magnetic data set (Luis and Miranda, 2008).

In contrast, younger structures like Monacco Bank (Fig. 5) or the active faults east of the Povoação Basin (Fig. 12) reveal a N160° orientation indicating a rotation in extension to N70°, which is the present-day extensional direction (DeMets et al., 2010; Luis and Miranda, 2008). This led to a rearrangement of the tectonic regime within the inherited N130° to N140° setting (Stage II, Fig. 14). West of São Miguel Island, the kinematics of the inherited faults probably changed from extension

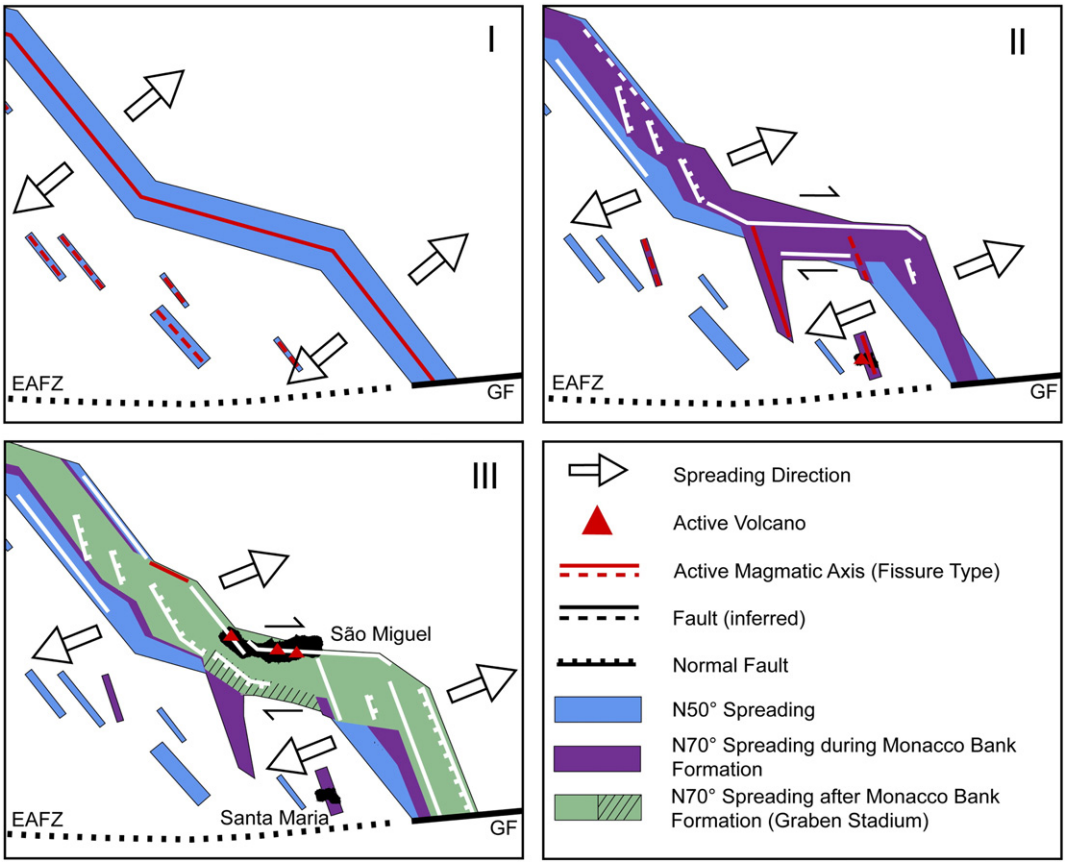

Fig. 14. Sketch of evolutionary stages of the southeastern Terceira Rift. Terceira Rift started to evolve under SW–NE rifting conditions ca. 25–20 Ma years ago. Fissure type magmatism occurred synchronously southwest of the plate boundary (I). After rifting has changed to WSW–ENE direction ca. 10 Ma years ago (II), Monacco Bank and early Santa Maria Island rose up. New faults west of São Miguel were formed in the inherited NW–SE setting. In the east, NNW–SSE trending faults developed. Ceasing magmatism at Monacco Bank at ~5 Ma led to the formation of Monacco Graben (III, graben stadium). Afterwards, extension was mainly accumulated by normal faulting in the southern Povoação Basin and its ancillary basin (III). Subaerial evolution of São Miguel Island started before 0.9 Ma. See Sections 5.2/5.3 for further details. EAFZ: East Azores Fracture Zone; GF: Gloria Fault.

to right-lateral transtension and new faults developed being clockwise rotated by 5°–15° (see faults in the South-Hirondelle Basin in Fig. 3). A similar phenomenon was discussed by Lourenço (2007) for southeast Terceira Island. Both, reactivated and new faults thus developed the N140° to N150° major trend that was described by Lourenço et al. (1998). Southeast of São Miguel, extension in the Povoação Basin decreased and Monacco Bank was formed south of the island, but Monacco Bank has never acted as an independent plate boundary since there is no connection to the East Azores Fracture Zone and Gloria Fault observed in the bathymetry. This possibly indicates Monacco Bank to be caused by a kind of fissure type volcanism as well — a further evidence for a formation linked to N70° extension.

After volcanic and tectonic processes at Monacco Bank had ceased, extension first accumulated north of it causing the opening of the oblique Monacco Graben (graben stadium of Stage III, Fig. 14). Then, tectonic stress again concentrated in the Povoação Basin (Stage III, Fig. 14), where it is still predominantly sustaining rifting along N160° faults. This thesis is in agreement with focal mechanisms presented by Borges et al. (2007) also describing present-day normal faulting here, although they obtained a more SW–NE direction of extension. In the South Basin, the transition from isotropic sedimentation conditions to an N–S directed sediment transport (S4 and S5 in Figs. 9–11, respectively) is assumed to indicate the time of subaerial exposure of São Miguel Island. Since Monacco Bank acts as a bathymetric barrier hampering a direct transport of material from São Miguel into the Southwest Basin, this transition cannot be traced there. Tectonic movements in the South Basin could be caused by rearrangement of the volcanic system associated with the major formation phase of São Miguel Island.

Distribution of present-day seismicity (Appendix 1), the absence of remarkable tectonic activity in the Monacco Graben (see Section 4.2.3) and the lack of active faults in the seismic/bathymetric data of the Southwest Basin and South Basin support the assumption that present-day extension accumulates along the South-Hirondelle Basin, São Miguel Island and the Povoação Basin only (Fernandes et al., 2006; Gente et al., 2003; Luis and Miranda, 2008; Vogt and Jung, 2004). In this context, the W–E trending central and eastern part of São Miguel Island seems to act as a kind of overstep structure that accommodates the offset between the reorganized fault setting of the Hirondelle domain and the "pure" N160° setting in the Povoação Basin. This could be caused by a deep rooted Eurasia/Nubia plate boundary related transtensional (leaky) transform. The associated extensional component could therefore facilitate the ascent of magma, which ultimately led to the formation of the volcanic body of São Miguel Island. Leaky transform faults and accompanying volcanism has been described by Favela and Anderson (2000) and references therein. A similar transform fault has also been discussed by Marques et al. (2014b) for the Pico-Faial area.

5.3. Age constrains

At 25–20 Ma, a major change in the kinematics of the Azores Triple Junction occurred when Iberia was finally welded to Eurasia (Luis and Miranda, 2008). This initiated the northward jump of the triple point and the evolution of the Terceira Axis. The subsequent rotation in extension from N50° to ~N70° (associated with horizon P) is stated to ~10 Ma (Luis and Miranda, 2008). This implies that formation of Monacco Bank started earliest at ~10 Ma (Table 1) and since a rock sample from the southern top of Monacco Bank was dated 5.9 Ma (Beier et al., 2015), it

was active at least until that time (horizon Q). (In this context, a second sample with an age of 39 Ma from the very northwest of Monacco Bank should be mentioned. According to magnetic data, the MAR was located in the area of São Miguel during that time (Gente et al., 2003; Luis and Miranda, 2008) casting the dating into doubt.)

Figs. 8 and 9 show a band of low reflection amplitudes with a thickness of ca. 180 ms at the base of units SW4/5 (Southwest Basin) and S4 (South Basin). This possibly corresponds with transparent upper Miocene hemipelagic sediments within the Atlantis Basin south of the Azores Plateau described by Alves et al. (2004). Hence, the top of the band could represent a time marker within the South Basin and Southwest Basin indicating that formation of the Monacco Bank and Graben ended prior the Pliocene (~5.3 Ma). However, difference in reflection amplitude is weak, less noticeable in the other two profiles covering the South Basin (Figs. 10/11) and possibly reflects attenuation of the seismic signal over depth only. In any case, the base of the Miocene unit cannot be inferred in the working area, since sedimentation during formation of Monacco Bank and Graben did not reflect hemipelagic sedimentation conditions.

Sibrant et al. (2015) recently postulated a change in the regional stress field of Santa Maria Island between 5.3 and 4.3 Ma, which was possibly linked to the ceasing tectonic activity at Monacco Graben (horizon R). According to this, the older part of the island evolved prior to 5.3 Ma and synchronously to the Monacco Bank and Monacco Graben.

Maximum ages of 0.9 Ma onshore São Miguel Island are reported by Johnson et al. (1998). Therefore, the subaerial island evolution started at or before that time (horizon S).

5.4. Implications for the Azores Plateau Evolution

The model presented above allows us to draw some general implications for the ongoing debate, whether the genesis of the Azores Plateau is driven by processes inside the upper mantle or if it is controlled by rigid tectonic plate kinematics.

The chronological order in the evolution of the N140° and N160° trending structural lineaments (and the intermediate trend), which could be correlated with modeled relative plate movements with extension in N50° and N70° directions, gives clear evidence that the tectonic and magmatic evolution of the Azores Plateau is strongly controlled by stress due to the differential plate movement of Nubia and Eurasia. This confirms the conclusion of Neves et al. (2013), who assume that mantle processes are eventually responsible for the high magma support, but arrangement and temporal evolution of the volcanic ridges are mainly driven by plate movements. Therefore, mantle convection may account for the initiation of the Terceira Rift (e.g. Gente et al., 2003; Yang et al., 2006), but it contradicts Adam et al. (2013) who argue stress induced by mantle upwelling being the prevalent factor for the tectonic regime. On the other hand, the dependency on plate movements shows that the evolution of the tectonic architecture is less forced by plate boundary effects as expected by Neves et al. (2013). However, plate boundary effects could account for the fact that the "pure" N160° trend solely developed at the outermost eastern pinnacle of the Azores Plateau.

Between Terceira and São Miguel, new faults with an intermediate orientation of N140°–160° evolved within the pre-existing N140° setting. This "new" trend is also described based on focal mechanisms (Miranda et al., 1998), bathymetric data (Lourenço et al., 1998) and data from onshore Terceira, where it is reflected by faults and volcanic lineaments interacting with mainly N110° trending structures (Lourenço, 2007; Montesinos et al., 2003; Navarro et al., 2003). Hence, N110° and N140°–N160° trending structures as described by Miranda et al. (1998) as well as inherited (N140°) and new faults (N145°–N160°) may define small isolated blocks, which possibly show minor clockwise rotation. This addresses the fact that sinistral seismicity along NNW–SSE rupture planes within an overall dextral setting has been recorded (Borges et al., 2007; Grimison and Chen, 1986; Hirn et al., 1980; Matias et al., 2007).

6. Conclusion

The southeastern Terceira Rift marks the Nubian–Eurasian plate boundary and comprises the South-Hirondelle Basin and the Povoação Basin. These basins are rift valleys whose southwestern and northeastern margins are defined by few major normal faults and several minor normal faults, respectively. In between, São Miguel Island presumably evolved above a leaky transform that links both basins. South of the island and separated by the N120° trending Monacco Graben system, the Monacco Bank represents a flat topped volcanic ridge dominated by tilted fault blocks.

Based on the characteristics of up to six seismic stratigraphic units per basin, a relative chronology of the tectonic and magmatic processes in the working area was deduced revealing three major stages (Table 1): I) the early volcano-tectonic evolution of N130°/N140 oriented structures before horizon P time, II) the formation of the N160° trending Monacco Bank, and III) the Post-Monacco-Bank stage including the formation of the Monacco Graben and the subaerial evolution of São Miguel after horizon Q times.

Referring to the more detailed stratigraphy of the Post-Monacco-Bank sediments and in consideration of published age data (Beier et al., 2015; Johnson et al., 1998; Luis and Miranda, 2008; Sibrant et al., 2015) and extension rates (DeMets et al., 2010; Luis and Miranda, 2008), we postulate a model for the volcano-tectonic evolution of the southeastern Terceira Rift. It includes the following steps:

- Volcano-tectonic evolution of the early Terceira Rift in a N50° orientated extensional setting (seismic units numbered "1"; I in Fig. 14).
- At ~10 Ma, rotation in extension to N70°. Subsequent formation of Monacco Bank (and early Santa Maria Island?). Rearrangement of the fault systems in the South Hirondelle Basin (seismic units numbered "2"; II in Fig. 14). Tectonics in the Povoação Basin decreased.
- At ≤ 5.9 Ma, formation of Monacco Bank ended. Subsequent opening of Monacco Graben (seismic units numbered "3"; III in Fig. 14, Graben Stadium).
- After rifting at Monacco Graben had ended (5.3–4.3 Ma?), tectonics of the Povoação Basin became reactivated. Uniform sedimentation during tectonic quiescence in the South Basin (seismic units numbered "4"; III in Fig. 14).
- At ≥ 0.9 Ma, subaerial evolution of São Miguel Island started initiating a N–S directed sediment flux into the South Basin. A possible rearrangement of the corresponding volcanic system caused minor tectonic activity in the South Basin at the beginning of this period (seismic units numbered "5"; III in Fig. 14).

Hence, the evolution of the southeastern Terceira Rift domain is predominantly controlled by plate kinematics and lithospheric stress forming a kind of a re-organized rift system.

Acknowledgments

We sincerely thank Captain Thomas Wunderlich and his outstanding crew of *RV Meteor* for their support during the M79/2 cruise. We are grateful for the financial support of the German Research Foundation (DFG, grant Hu698/19-1). Additional acknowledgments go to the companies Halliburton-Landmark and Schlumberger for providing university grants for the seismic processing software ProMAX and seismic interpretation software Petrel, respectively, as well as to the NASA's Earth Science Data Systems program for providing the ASTER Global DEM data. Special thanks go to Sönke Reiche for all the helpful discussions. Finally, we want to thank F.O. Marques and N.C. Mitchell for reviewing the manuscript. Their suggestions helped a lot to enhance the quality of this publication.

Appendix 1. Recorded seismicity since 1900

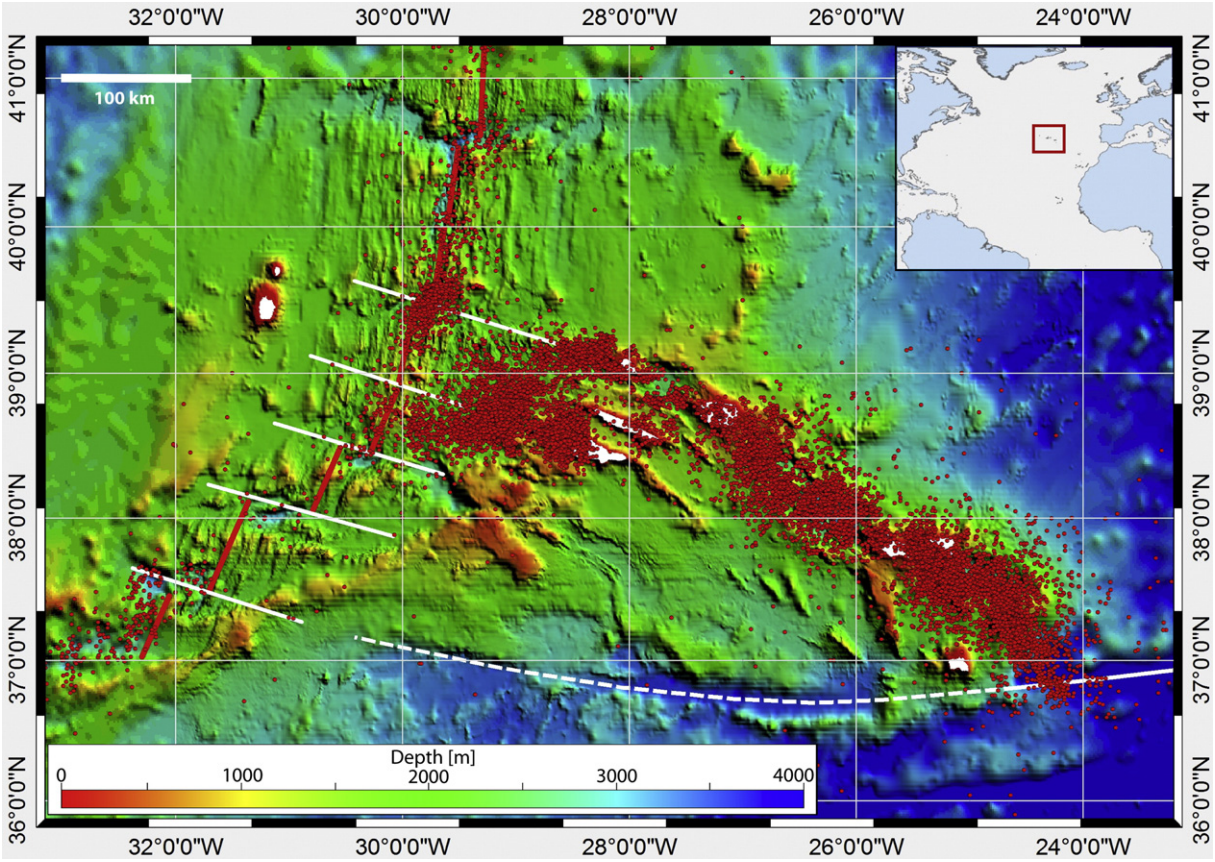

Data from International Seismological Centre (2012). Since the magnitude is known for the younger events only, they are shown without any threshold applied.

Appendix 2. Simplified fault map of the working area

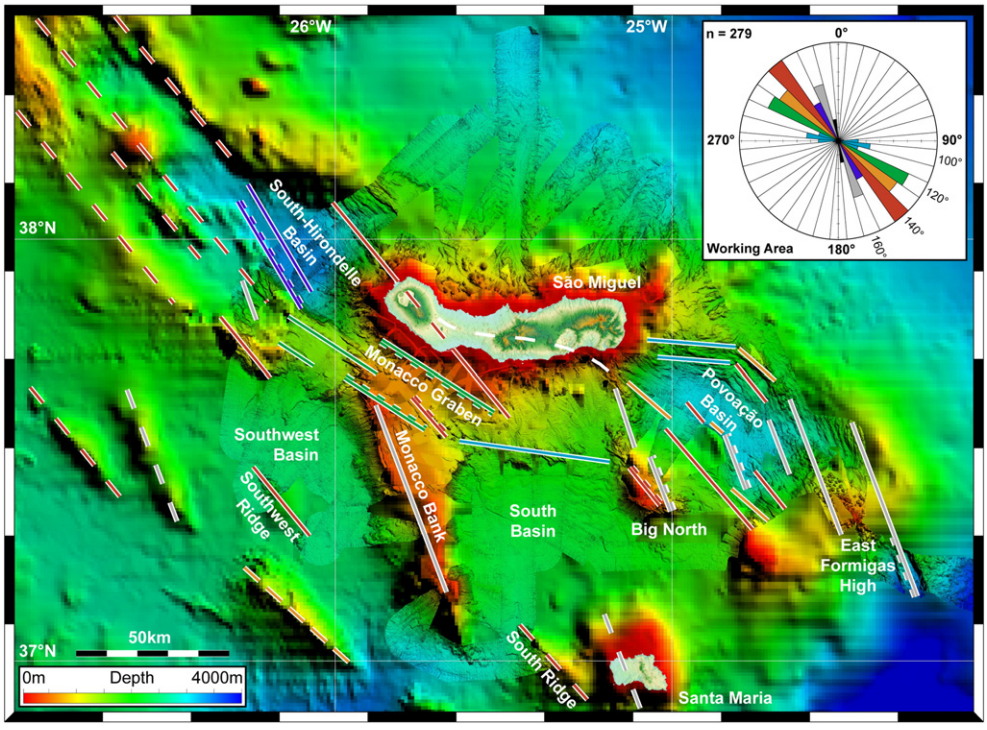

Normal faults symbol denotes areas with major vertical offset. Colored dashed lines indicate trends inferred based on bathymetric data published by Lourenço et al. (1998), which are not considered in the rose diagram. White dashed line represents major onshore trends (after Carmo (2004), Ferreira (2000), Guest et al. (1999), Queiroz (1997)).

References

Adam, C., et al., 2013. Mantle dynamics and characteristics of the Azores Plateau. Earth Planet. Sci. Lett. 258–271 http://dx.doi.org/10.1016/j.epsl.2012.11.014 (Band 362).

Alves, T., et al., 2004. Surveying the flanks of the Mid-Atlantic Ridge: the Atlantis Basin, North Atlantic Ocean (36°N). Mar. Geol. 209 (1–4), 199–222. http://dx.doi.org/10.1016/j.margeo.2004.06.002.

Amante, C., Eakins, B.W., 2009. ETOPO1 1 Arc-minute Global Relief Model: Procedures, Data Sources and Analysis (19 pp., NOAA Technical Memorandum NESDIS NGDC-24).

Asimow, P.D., Dixon, J.E., Langmuir, C.H., 2004. A hydrous melting and fractionation model for mid-ocean ridge basalts: application to the Mid-Atlantic Ridge near the Azores. Geochem. Geophys. Geosyst. 5 (1). http://dx.doi.org/10.1029/2003GC000568.

Beier, C., et al., 2008. Magma genesis by rifting of oceanic lithosphere above anomalous mantle: Terceira Rift, Azores. Geochem. Geophys. Geosyst. 9 (12). http://dx.doi.org/10.1029/2008GC002112.

Beier, C., Haase, K.M., Abouchami, W., 2015. Geochemical and geochronological constraints on the evolution of the Azores Plateau. In: Neal, C.R., Sager, W., Erba, E., Sano, T. (Eds.), The Origin, Evolution, and Environmental Impact of Oceanic Large Igneous Provinces. Geol. Soc. Am. Spec. Pap 511, pp. 1–29. http://dx.doi.org/10.1130/2015.2511(02).

Bonatti, E., 1990. Not so hot "hot spots" in the oceanic mantle. Science 250 (4977), 107–111. http://dx.doi.org/10.1126/science.250.4977.107.

Borges, J., et al., 2007. The 1980, 1997 and 1998 Azores earthquakes and some seismotectonic implications. Tectonophysics 435 (1–4), 37–54. http://dx.doi.org/10.1016/j.tecto.2007.01.008.

Bourdon, B., Turner, S.P., Ribe, N.M., 2005. Partial melting and upwelling rates beneath the Azores from a U-series isotope perspective. Earth Planet. Sci. Lett. 239 (1–2), 42–56. http://dx.doi.org/10.1016/j.epsl.2005.08.008.

Buforn, E., Udías, A., Colombás, M.A., 1988. Seismicity, source mechanisms and tectonics of the Azores-Gibraltar plate boundary. Tectonophysics 152 (1-2), 89–118. http://dx.doi.org/10.1016/0040-1951(88)90031-5.

Bull, S., Cartwright, J., Huuse, M., 2009. A review of kinematic indicators from mass-transport complexes using 3D seismic data. Mar. Pet. Geol. 26 (7), 1132–1151. http://dx.doi.org/10.1016/j.marpetgeo.2008.09.011.

Cannat, M., et al., 1999. Mid-Atlantic Ridge–Azores hotspot interactions: along-axis migration of a hotspot-derived event of enhanced magmatism 10 to 4 Ma ago. Earth Planet. Sci. Lett. 173 (3), 257–269. http://dx.doi.org/10.1016/S0012-821X(99)00234-4.

Carmo, R., 2004. Geologia estrutural da região Povoação - Nordeste (ilha de S. Miguel, Açores). Tese de Mestrado em Vulcanologia e Avaliação de Riscos Geológicos, Departamento de Geociências, Universidade dos Açores (121 pp.).

Carvalho, M., Forjaz, V., Almeida, C., 2006. Chemical composition of deep hydrothermal fluids in the Ribeira Grande geothermal field (São Miguel, Azores). J. Volcanol. Geotherm. Res. 156 (1–2), 116–134. http://dx.doi.org/10.1016/j.jvolgeores.2006.03.015.

DeMets, C., Gordon, R.G., Argus, D.F., 2010. Geologically current plate motions. Geophys. J. Int. 181 (1), 1–80. http://dx.doi.org/10.1111/j.1365-246X.2009.04491.x.

Detrick, R.S., Needham, H.D., Renard, V., 1995. Gravity anomalies and crustal thickness variations along the Mid-Atlantic Ridge between 33°N and 40°N. J. Geophys. Res. Solid Earth 100 (B3), 3767–3787. http://dx.doi.org/10.1029/94JB02649.

Dias, N., et al., 2007. Crustal seismic velocity structure near Faial and Pico Islands (AZORES), from local earthquake tomography. Tectonophysics 445 (3–4), 301–317. http://dx.doi.org/10.1016/j.tecto.2007.09.001.

Escartín, J., et al., 2001. Crustal thickness of V-shaped ridges south of the Azores: interaction of the Mid-Atlantic Ridge (36°–39°N) and the Azores hot spot. J. Geophys. Res. 106 (B10), 21719–21735. http://dx.doi.org/10.1029/2001JB000224.

Favela, J., Anderson, D.L., 2000. Extensional tectonics and global volcanism. Problems in Geophysics for the New Millennium. Editrice Compositori Bologna, pp. 463–498.

Fernandes, R., et al., 2006. Defining the plate boundaries in the Azores region. J. Volcanol. Geotherm. Res. 156 (1–2), 1–9. http://dx.doi.org/10.1016/j.jvolgeores.2006.03.019.

Ferreira, T., 2000. Caracterização da actividade vulcânica da ilha de S. Miguel (Açores): vulcanismo basáltico recente e zonas de desgasificação. Avaliação de riscos. Departamento de Geociências da Universidade dos Açores.

Gente, P., Dyment, J., Maia, M., Goslin, J., 2003. Interaction between the Mid-Atlantic Ridge and the Azores hot spot during the last 85 Myr: emplacement and rifting of the hot spot-derived plateaus. Geochem. Geophys. Geosyst. 4 (10). http://dx.doi.org/10.1029/2003GC000527.

Georgen, J.E., Sankar, R.D., 2010. Effects of ridge geometry on mantle dynamics in an oceanic triple junction region: implications for the Azores Plateau. Earth Planet. Sci. Lett. 298 (1–2), 23–34. http://dx.doi.org/10.1016/j.epsl.2010.06.007.

Grimison, N.L., Chen, W.-P., 1986. The Azores–Gibraltar Plate Boundary: focal mechanisms, depths of earthquakes, and their tectonic implications. J. Geophys. Res. Solid Earth 91 (B2), 2029–2047. http://dx.doi.org/10.1029/JB091iB02p02029.

Guest, J., et al., 1999. Volcanic geology of Furnas Volcano, São Miguel, Azores. J. Volcanol. Geotherm. Res. 92 (1–2), 1–29. http://dx.doi.org/10.1016/S0377-0273(99)00064-5.

Hildenbrand, A., Weis, D., Madureira, P., Marques, F.O., 2014. Recent plate re-organization at the Azores Triple Junction: evidence from combined geochemical and geochronological data on Faial, S. Jorge and Terceira volcanic islands. Lithos 210–211 (0), 27–39. http://dx.doi.org/10.1016/j.lithos.2014.09.009.

Hirn, A., et al., 1980. Aftershock sequence of the January 1st, 1980, earthquake and present-day tectonics in the Azores. Geophys. Res. Lett. 7 (7), 501–504. http://dx.doi.org/10.1029/GL007i007p00501.

Hübscher, C., 2013. Tragica — Cruise No. M79/2 — August 26–September 21, 2009. Ponta Delgada (Azores/Portugal) — Las Palmas (Canary Islands/Spain). *METEOR-Berichte, M79/2*. DFG-Senatskommission für Ozeanographie (37 pp., https://getinfo.de/app/details?id=awi:doi~10.2312%252Fcr_m79_2).

International Seismological Centre, 2012. On-line Bulletin, Thatcham, United Kingdom.

Johnson, C.L., et al., 1998. $^{40}Ar/^{39}Ar$ ages and paleomagnetism of São Miguel lavas, Azores. Earth Planet. Sci. Lett. 160 (3–4), 637–649. http://dx.doi.org/10.1016/S0012-821X(98)00117-4.

Krause, D.C., Watkins, N.D., 1970. North Atlantic crustal genesis in the vicinity of the Azores. Geophys. J. Int. 19 (3), 261–283. http://dx.doi.org/10.1111/j.1365-246X.1970.tb06046.x.

Ligi, M., et al., 1999. Bouvet Triple Junction in the South Atlantic: geology and evolution. J. Geophys. Res. Solid Earth 104 (B12), 29365–29385. http://dx.doi.org/10.1029/1999JB900192.

Lourenço, N., 2007. Tectonono-Magmatic Processes at the Azores Triple Junction. Universidade Do Algarve.

Lourenço, N., et al., 1998. Morpho-tectonic analysis of the Azores Volcanic Plateau from a new bathymetric compilation of the area. Mar. Geophys. Res. 141–156 (Band 20).

Luis, J.F., Miranda, J.M., 2008. Reevaluation of magnetic chrons in the North Atlantic between 35°N and 47°N: implications for the formation of the Azores Triple Junction and associated plateau. J. Geophys. Res. Solid Earth http://dx.doi.org/10.1029/2007JB005573 (Band 113).

Luis, J., Neves, M., 2006. The isostatic compensation of the Azores Plateau: a 3D admittance and coherence analysis. J. Volcanol. Geotherm. Res. 10–22 (Band 156).

Luis, J.F., et al., 1994. The Azores triple junction evolution since 10 Ma from an aeromagnetic survey of the Mid-Atlantic Ridge. Earth Planet. Sci. Lett. 125 (1–4), 439–459. http://dx.doi.org/10.1016/0012-821X(94)90231-3.

Luis, J., Miranda, J., Galdeano, A., Patriat, P., 1998. Constraints on the structure of the Azores spreading center from gravity data. Mar. Geophys. Res. 20 (3), 157–170.

Marques, F., et al., 2013. GPS and tectonic evidence for a diffuse plate boundary at the Azores Triple Junction. Earth Planet. Sci. Lett. 381 (0), 177–187. http://dx.doi.org/10.1016/j.epsl.2013.08.051.

Marques, F., et al., 2014a. Corrigendum to "GPS and tectonic evidence for a diffuse plate boundary at the Azores Triple Junction" [Earth Planet. Sci. Lett. 381 (2013) 177–187]. Earth Planet. Sci. Lett. 387 (1), 1–3. http://dx.doi.org/10.1016/j.epsl.2013.11.029.

Marques, F., et al., 2014b. The 1998 Faial earthquake, Azores: evidence for a transform fault associated with the Nubia–Eurasia plate boundary? Tectonophysics 633, 115–125.

Matias, L., et al., 2007. The 9th of July 1998 Faial Island (Azores, North Atlantic) seismic sequence. J. Seismol. 11 (3), 275–298. http://dx.doi.org/10.1007/s10950-007-9052-4.

McKenzie, D., 1972. Active tectonics of the Mediterranean region. Geophys. J. Int. 30 (2), 109–185. http://dx.doi.org/10.1111/j.1365-246X.1972.tb02351.x.

Métrich, N., et al., 2014. Is the 'Azores hotspot' a wetspot? Insights from the geochemistry of fluid and melt inclusions in olivine of Pico Basalts. J. Petrol. 55 (2), 377–393. http://dx.doi.org/10.1093/petrology/egt071.

Miranda, J., et al., 1998. Tectonic setting of the Azores Plateau deduced from a OBS survey. Mar. Geophys. Res. 20 (3), 171–182. http://dx.doi.org/10.1023/A%3A1004622825210.

Miranda, J., Luis, J., Lourenço, N., Goslin, J., 2014. Distributed deformation close to the Azores Triple "Point". Mar. Geol. 355 (0), 27–35. http://dx.doi.org/10.1016/j.margeo.2014.05.006.

Mitchell, N.C., Livermore, R.A., Fabretti, P., Carrara, G., 2000. The Bouvet triple junction, 20 to 10 Ma, and extensive transtensional deformation adjacent to the Bouvet and Conrad transforms. J. Geophys. Res. Solid Earth 105 (B4), 8279–8296. http://dx.doi.org/10.1029/1999JB900399.

Mitchell, N., et al., 2012. Cone morphologies associated with shallow marine eruptions: east Pico Island, Azores. Bull. Volcanol. 74 (10), 2289–2301. http://dx.doi.org/10.1007/s00445-012-0662-5.

Montelli, R., Nolet, G., Dahlen, F.A., Masters, G., 2006. A catalogue of deep mantle plumes: new results from finite-frequency tomography. Geochem. Geophys. Geosyst. 7 (11). http://dx.doi.org/10.1029/2006GC001248.

Montesinos, F.G., et al., 2003. A 3-D gravity model for a volcanic crater in Terceira Island (Azores). Geophys. J. Int. 154 (2), 393–406. http://dx.doi.org/10.1046/j.1365-246X.2003.01960.x.

Navarro, A., Catalao, J., Miranda, J.M., Fernandes, R.M., 2003. Estimation of the Terceira Island (Azores) main strain rates from GPS data. Earth Planets Space 55 (10), 637–642.

Navarro, A., et al., 2009. Analysis of geometry of volcanoes and faults in Terceira Island (Azores): evidence for reactivation tectonics at the EUR/AFR plate boundary in the Azores triple junction. Tectonophysics 465 (1–4), 98–113. http://dx.doi.org/10.1016/j.tecto.2008.10.020.

Neves, M., Miranda, J., Luis, J., 2013. The role of lithospheric processes on the development of linear volcanic ridges in the Azores. Tectonophysics 608 (0), 376–388. http://dx.doi.org/10.1016/j.tecto.2013.09.016.

Queiroz, G., 1997. Vulcão das Sete Cidades (S. Miguel, Açores): história eruptiva e avaliação do hazard. Tese de Doutoramento em Geologia na especialidade de Vulcanologia, Departamento de Geociências da Universidade dos Açores (226 pp.).

Rebesco, M., Hernández-Molina, F.J., Rooij, D.V., Wåhlin, A., 2014. Contourites and associated sediments controlled by deep-water circulation processes: state-of-the-art and future considerations. Mar. Geol. 352 (0), 111–154. http://dx.doi.org/10.1016/j.margeo.2014.03.011.

Schilling, J.-G., 1975. Azores mantle blob: rare-earth evidence. Earth Planet. Sci. Lett. 25 (2), 103–115. http://dx.doi.org/10.1016/0012-821X(75)90186-7.

Schilling, J.-G., 1985. Upper mantle heterogeneities and dynamics. Nature 62–67 http://dx.doi.org/10.1038/314062a0 (March, Band 314).

Schilling, J.-G., Bergeron, M.B., Evans, R., Smith, J.V., 1980. Halogens in the mantle beneath the North Atlantic [and discussion]. Philos. Trans. R. Soc. Lond. Ser. A Math. Phys. Sci. 297 (1431), 147–178. http://dx.doi.org/10.1098/rsta.1980.0208.

Searle, R., 1980. Tectonic pattern of the Azores spreading centre and triple junction. Earth Planet. Sci. Lett. 51 (2), 415–434. http://dx.doi.org/10.1016/0012-821X(80)90221-6.

Sibrant, A., Hildenbrand, A., Marques, F., Costa, A., 2015. Volcano-tectonic evolution of the Santa Maria Island (Azores): implications for paleostress evolution at the western Eurasia–Nubia plate boundary. J. Volcanol. Geotherm. Res. 291 (0), 49–62. http://dx.doi.org/10.1016/j.jvolgeores.2014.12.017.

Silveira, G., et al., 2006. Azores hotspot signature in the upper mantle. J. Volcanol. Geotherm. Res. 156 (1–2), 23–34. http://dx.doi.org/10.1016/j.jvolgeores.2006.03.022.

Silveira, G., et al., 2010. Stratification of the Earth beneath the Azores from P and S receiver functions. Earth Planet. Sci. Lett. 299 (1–2), 91–103. http://dx.doi.org/10.1016/j.epsl.2010.08.021.

Srivastava, S., et al., 1990. Motion of Iberia since the Late Jurassic: results from detailed aeromagnetic measurements in the Newfoundland Basin. Tectonophysics 184 (3–4), 229–260. http://dx.doi.org/10.1016/0040-1951(90)90442-B.

Stretch, R., Mitchell, N., Portaro, R., 2006. A morphometric analysis of the submarine volcanic ridge south-east of Pico Island, Azores. J. Volcanol. Geotherm. Res. 156 (1–2), 35–54. http://dx.doi.org/10.1016/j.jvolgeores.2006.03.009.

Thibaud, R., Gente, P., Maia, M., 1998. A systematic analysis of the Mid-Atlantic Ridge morphology and gravity between 15°N and 40°N: constraints of the thermal structure. J. Geophys. Res. Solid Earth 103 (B10), 24223–24243. http://dx.doi.org/10.1029/97JB02934.

Udías, A., Arroyo, A., Mezcua, J., 1976. Seismotectonic of the Azores–Alboran region. Tectonophysics 31 (3–4), 259–289. http://dx.doi.org/10.1016/0040-1951(76)90121-9.

Vogt, P., Jung, W., 2004. The Terceira Rift as hyper-slow, hotspot-dominated oblique spreading axis: a comparison with other slow-spreading plate boundaries. Earth Planet. Sci. Lett. 218 (1–2), 77–90. http://dx.doi.org/10.1016/S0012-821X(03)00627-7.

White, W.M., Schilling, J.-G., 1978. The nature and origin of geochemical variation in Mid-Atlantic Ridge basalts from the Central North Atlantic. Geochim. Cosmochim. Acta 42 (10), 1501–1516. http://dx.doi.org/10.1016/0016-7037(78)90021-2.

Yang, T., et al., 2006. Upper mantle structure beneath the Azores hotspot from finite-frequency seismic tomography. Earth Planet. Sci. Lett. 250 (1–2), 11–26. http://dx.doi.org/10.1016/j.epsl.2006.07.031.